Optimizing Reactive Power Dispatch in Electrical Networks Using a Hybrid Artificial Rabbits and Gradient-Based optimization

Ahmed M. Abd-El Wahab[1], Salah Kamel[1], Hamdy M. Sultan[2], Mohamed H. Hassan[3], Francisco J. Ruiz-Rodríguez[4, *]

[1]Department of Electrical Engineering, Faculty of Engineering, Aswan University, Aswan 81542, Egypt

[2]Department of Electrical Engineering, Faculty of Engineering, Minia University, Minia 61517, Egypt

[3]Ministry of Electricity and Renewable Energy, Cairo, Egypt

[4]Department of Electrical and Thermal Engineering, School of Engineering, University of Huelva, Huelva 21007, Spain;

eng8080_ahmed@yahoo.com, skamel@aswu.edu.eg, hamdy.soltan@mu.edu.eg, mohamedhosnymoee@gmail.com, javier.ruiz@die.uhu.es

Abstract

The optimal reactive power dispatch (ORPD) problem is a critical factor in maintaining the safe and efficient operation of electric networks. Due to its mixed-variable nonlinear nature, addressing this problem requires an appropriate optimization algorithm. In this study, a novel approach based on the combination of Artificial Rabbits Optimization (ARO) and gradient-based optimization (GBO) algorithms was proposed to solve the ORPD problem in electric networks. The performance of the proposed AROGBO algorithm were verified on 7 numerical optimization test functions. To evaluate the effectiveness of this hybrid AROGBO technique, standard IEEE-30, IEEE-57 bus, and IEEE-118 bus test systems were employed, with two objective functions tested for each system: minimum total power loss and minimum total voltage deviations. The AROGBO, ARO, and GBO algorithms were utilized in each case to determine the optimal values of the generator voltage, transformer tap changer positions, and reactive power compensation values. A comprehensive comparison was made between the results obtained from the hybrid AROGBO algorithm, standard ARO and GBO algorithms, and other metaheuristic optimization techniques. The simulation attainments verify the accuracy and stability of the proposed AROGBO methodology in solving the ORPD problem.

Keywords: *Optimal Reactive Power Dispatch ORPD; Artificial Rabbits Optimization (ARO): Gradient based optimizer (GBO); Active power losses; Voltage deviation.*

1. Introduction

Optimizing reactive power dispatch (ORPD) has become a crucial concern for researchers in the field of electric energy management. The main aim of this problem is to minimize actual power losses in the system, increase bus voltage magnitude, and satisfy capacity requirements and operational constraints [1, 2]. ORPD is a nonlinear and complex optimization problem that involves both dependent and independent variables, representing equality and inequality constraints. To achieve the desired objectives, various control variables such as transformer tap changer settings, voltage magnitude at generator buses, and reactive power generation from shunt capacitor banks need to be optimally adjusted. Throughout the optimization process, both equality and inequality constraints must be maintained within their accepted upper and lower limits [3].

The primary objective of ORPD is to enhance the voltage profile by reducing the total voltage deviations (TVD) at load buses from the reference value, minimize the total real power losses (Ploss) in the system, and reduce the cost of shunt reactive power compensators. Over the years, several mathematical optimization techniques have been developed and utilized to address this issue. However, these traditional methods have limitations, especially when dealing with nonlinear complex problems such as ORPD that involve discrete variables in the objective function, requiring numerous iterations and lengthy calculations to reach the optimal solution [4]. As a result, recent optimization methodologies have been developed, and different optimization solvers have been employed to tackle several power system problems, including the ORPD problem, to overcome these challenges.

In the past few years, the effectiveness of metaheuristic algorithms (MA) in addressing the ORPD problem has been widely observed. Various MA optimization algorithms have been employed to tackle this problem. These algorithms have incorporated a diverse set of single objective functions, such as minimizing real power loss, reducing total voltage deviations, optimizing system operational cost, minimizing fuel cost, improving voltage stability index, and integrating these objectives into a multi-objective function.

In [6], the firefly algorithm (FA) was applied to the IEEE 14 Bus system with load uncertainty and incorporated the objective functions of minimizing total power losses and voltage deviations. The chaotic turbulent flow of water-based optimization (CTFWO) method was employed in [7] to solve the ORPD problem in the IEEE 30-Bus and IEEE 57-Bus systems with the objective of minimizing Ploss and TVD. An improved differential evolution (IDE) algorithm was used in [8] to address the ORPD issue in the IEEE 14-Bus and IEEE 30-Bus systems with the objective of minimizing total power losses.

Finally, in [9], a novel inertia weight strategy of Particle Swarm Optimization (PSO) was employed to tackle the RPD optimization problem in the IEEE 14-Bus system with the objective of minimizing P_{loss}. In [10], the modified coyote optimization algorithm (MCOA) was used to address the ORPD issue in IEEE 14-Bus, IEEE 57-Bus, and IEEE 118-Bus test systems with different objective functions such as minimizing power losses, voltage deviations, and improving power stability index. In [11], the moth-flame optimizer (MFO) was applied to IEEE 30-Bus, IEEE 57-Bus, and IEEE 118-Bus test systems to minimize total voltage deviations and power losses as single objective functions. Quasi-oppositional differential evolution (QODE) was utilized in [12] to address the ORPD issue, while in [13], the Rao-3 optimization methodology was developed for minimizing P_{loss} and VD as objective functions in IEEE 57-Bus and IEEE 118-Bus test systems with uncertainties of distributed generators. The JAYA algorithm was used in [14] to address the ORPD issue in IEEE 14-Bus, IEEE 30-Bus, IEEE 57-Bus, and IEEE 118-Bus test systems with the objective of reducing P_{loss}. In [15], a modified JAYA algorithm was employed to address the ORPD issue in IEEE 30-Bus and IEEE 57-Bus test systems while considering load uncertainties and using two single fitness functions: minimizing P_{loss} and minimizing VD.

Moreover, in [16], Mean-Variance Mapping Optimization Algorithm (MVMO) was employed for optimal RPD in IEEE 30-Bus and IEEE 57-Bus test systems while the reduction of P_{loss} is the objective function. In [17], a modified Heap-based optimizer (MHBO) has been applied for ORPD in IEEE 30-Bus, IEEE 57-Bus, and IEEE 118-Bus and utilizing minimization of P_{loss}, minimization of VD, and enhancement of stability index as different single objective functions. In [18], the ORPD problem was solved in IEEE 30-Bus and IEEE 57-Bus networks using the chaotic krill herd algorithm (CKHA). In [19], a multi-objective PSO (MOPSO) was used to address the reactive power dispatch issue in IEEE 14-Bus and IEEE 30-Bus systems by minimizing both P_{loss} and VD. In [20], the hybrid grey wolf optimizer and PSO (GWO-PSO) were applied to IEEE 14-Bus, IEEE 30-Bus, and IEEE 118-Bus systems to minimize VD and Ploss for optimal RPD. The marine predators' algorithm (MPA) was employed in [21] to address the ORPD problem on the IEEE 30-Bus system while considering unpredictable load demand and power from distributed renewable sources. The water wave optimization (WWO) was utilized in [22] to minimize active power losses in lines for optimal RPD in IEEE 30-Bus. The pathfinder algorithm (PFA) was employed in [23] to achieve minimum power losses in IEEE 57-Bus and IEEE 118-Bus systems. Finally, the ORPD problem on IEEE 30-Bus, IEEE 57-Bus, and IEEE 118-Bus systems was addressed using feasible solutions differential evolution (FS-ED), self-adaptive penalty differential evolution (SP-DE), ε-constraint differential evolution (EC-DE), stochastic ranking

differential evolution (SR-DE), and the ensemble of constraint handling techniques differential evolution (ECHT-DE) in [24].

In [25], the hybrid PSO with firefly algorithm (HPSOFA) was applied to minimize power losses and voltage deviations in IEEE 14-Bus and IEEE 30-Bus systems. Fractional particle swarm optimization gravitational search algorithm (FPSOGSA) was utilized in [26, 27] to achieve minimum Ploss and VD in IEEE 30-Bus and IEEE 57-Bus test systems. In [28], the proposed technique considered uncertainty in distributed sources and load demand to achieve minimum Ploss, minimum VD, and improve voltage stability index. Particle swarm optimization (PSO) was used in [29] to address the ORPD issue with total cost minimization and total power loss minimization as single objective functions in IEEE 30-Bus test system. Simplified sine cosine algorithm (SSCA) was applied in [30] to minimize line losses and maximize earnings in IEEE 30-Bus, IEEE 57-Bus, and IEEE 118-Bus test systems. Lightning attachment procedure optimization (LAPO) was utilized in [31] to minimize Ploss and VD in IEEE 30-Bus test system while considering uncertainty in load demand and distributed generation. Improved social spider optimization (ISSO) was used in [32] to achieve different objectives such as minimizing Ploss, minimizing VD, and enhancing voltage stability index in IEEE 30-Bus and IEEE 118-Bus test systems. In [33], chaotic bat algorithm (CBA) was employed in various power systems, including IEEE 14-Bus, IEEE 57-Bus, IEEE 118-Bus, and IEEE 300-Bus test systems, to achieve minimum Ploss, minimum VD, and enhance voltage stability index.

Wang et al. developed Artificial Rabbits Optimization (ARO) which imitates the survival behavior of rabbits [34]. ARO has demonstrated its superiority over classical and recent optimization algorithms in solving various benchmark and real engineering problems. The excellent performance of ARO motivated researchers to modify and develop the original algorithm and apply it to different complex engineering problems [35, 36]. Another optimization algorithm, Gradient Based Optimizer (GBO), was proposed by Ahmadianfar et al., and is inspired by the gradient-based Newton's method [37]. According to the results presented in [37], the GBO methodology has promising performance compared to well-known optimization algorithms due to its better capability in the exploration and exploitation phases and its ability to escape from falling into local optima. The improved behavior of GBO has attracted researchers to validate it in addressing complex nonlinear engineering problems such as parameters extraction of solar cells [38], economic load dispatch [39], and parameter estimation of proton exchange membrane fuel cells [40].

The impressive performance of both ARO and GBO algorithms has motivated us to create a hybrid method that combines the advantages of both algorithms. The modified hybrid AROGBO algorithm has been applied to standard IEEE 30-Bus and IEEE 57-Bus test systems to evaluate its effectiveness in solving the ORPD optimization problem. The fitness functions used in this study are the minimization of total power losses in the lines (Ploss) and the minimization of the total deviations of bus voltage (VD) from the reference value. These objective functions are applied as single objective functions. Based on the results, the developed hybrid AROGBO method has shown superiority over other metaheuristic algorithms. In summary, the main achievements of this study are as follows:

- ✓ Development of a hybrid AROGBO algorithm that combines the strengths of ARO and GBO algorithms.
- ✓ The robustness of the developed hybrid AROGBO method in solving seven benchmark optimization functions is validated through a comparison with ARO and GBO methods.
- ✓ Validation of the robustness of the developed hybrid AROGBO method for solving the ORPD problem and achieving minimum P_{loss} and minimum VD.
- ✓ Evaluation of the accuracy of the developed hybrid AROGBO method using the IEEE 30-Bus, IEEE 57-Bus and IEEE 118-Bus test systems.
- ✓ Statistical analysis to compare the accuracy and robustness of the developed AROGBO algorithm with the standard ARO and GBO algorithms.
- ✓ Comparison of the performance of the developed hybrid AROGBO algorithm with recent metaheuristic algorithms, demonstrating promising results.

The paper is organized as follows: Section 2 presents an overview of the ORPD problem, Section 3 describes the development of the hybrid AROGBO algorithm, as well as the original ARO and GBO algorithms, Section 4 presents simulation results and discussions, and Section 5 concludes the study's main findings.

2. ORPD Problem Formulation

The objective of the ORPD problem is to achieve optimal results by appropriately modifying the control variables of the power system, while considering various equality and inequality constraints. Typically, this optimization process can be expressed using the objective function described in equation (1).

$$\text{minimize } f(x,u)$$
$$\text{subject to } \begin{cases} A_m(x,u) = 0 & m = 1,\ldots,j \\ B_m(x,u) \leq 0 & m = 1,\ldots k \end{cases} \quad (1)$$

The equation for the objective function is represented as Eq. (1), where the state variables vector is denoted as *x* and the control variables vector is denoted as *u*. The equality constraints are represented by A_m, and the inequality constraints are represented by Bm. The length of the equality and inequality constraints are represented by j and k, respectively. The dependent variables are formulated in Eq. (2), while the independent variables are presented in Eq. (3).

$$x = [P_{G1}, V_{L,1} \ldots\ldots V_{L,NL}, Q_{G,1}, \ldots Q_{G,NG}, S_{TL,1}, \ldots S_{TL,NTL}] \quad (2)$$

where P_{G1}symbolizes the power of the slack bus, V_L signifies the values of the voltage at the load bus, Q_G denotes the reactive power supplied by the generator, S_{TL} symbolizes the flow of apparent power via the transmission line. The symbols NL, NG, and NTL, respectively, stand for the number of loads, generators, and transmission lines.

$$u = [P_{G,2}, \ldots, P_{G,NG}, V_{G1} \ldots\ldots V_{G,NG}, Q_{C,1}, \ldots Q_{C,NC}, T_1, \ldots T_{NT}] \quad (3)$$

where P_G denotes the real power supplied by the generating plant, V_G denotes the value of the voltage magnitude at the generator buses, Q_C symbolizes the reactive power supplied by the shunt compensators, T symbolizes the setting of the tap changer of the transformer. NG, NC, and NT signify the number of generators, shunt capacitors and transformers.

2.1. Objective Functions

In this study, the total voltage deviation (TVD) and total active power loss (P_{loss}) were combined into a single objective function.

- Minimization of Real Power Loss

From an economic perspective, electric energy suppliers must ensure a consistent supply of active power and maintain the transmission line capacity. Thus, minimizing power losses in transmission line sections is crucial for power system operators. The minimization of power losses can be formulated as follows.

$$f_1 = \min(P_{loss})$$

$$f_1 = \min\left[\sum_{i=1}^{\mathrm{NTL}} g_{ij}\left(V_i^2 + V_j^2 - 2V_iV_j\ \cos\alpha_{ij}\right)\right] \quad (4)$$

where V_i , V_j signify the voltage magnitude at ith and jth buses respectively, α_{ij} denotes the phase difference between the voltage angles, and g_{ij}symbolizes the conductance of the branch between ith and jth nodes.

- Minimization of voltage deviation

In contemporary power systems, voltage instability has become a major concern that requires investigation to ensure a reliable power supply. The deviation of voltage at each load bus from its designated base is computed. To evaluate the voltage stability of the power system, the sum of these voltage deviations is expressed as an objective function that needs to be minimized. The formulation for minimizing voltage deviations (VD) can be expressed as follows:

$$f_2 = min(VD)$$

$$f_2 = \min\left(\sum_{i=1}^{\mathrm{NL}} |V_i - 1|\right) \quad (5)$$

where V_i denotes the voltage magnitude at the i^{th} load bus [26, 27].

2.2. System Constraints

- Equality Constraint

Equality constraints are represented by the real and reactive power balance and are expressed as follow:

$$P_{Gi}\ -\ P_{Di} - |V_i|\sum_{j=1}^{\mathrm{NB}}|\mathrm{V_j}|\left[G_{ij}\cos\alpha_{ij} + B_{ij}\sin\alpha_{ij}\right] = 0 \quad (6)$$

$$Q_{Gi} - Q_{Di} - |V_i| \sum_{j=1}^{\mathrm{NB}} \left|\mathrm{V_j}\right| \left[G_{ij} \sin \alpha_{ij} - B_{ij} \cos \alpha_{ij}\right] = 0 \qquad (7)$$

where P_{Gi} and Q_{Gi} signify the real and reactive power injection at bus i. P_{Di} and Q_{Di} signify the real and reactive power drawn by the load at bus i, respectively. B_{ij} is the susceptance of the branch between bus i and bus j, N_B denotes the total number of buses.

- Inequality Constraints

The inequality constraints describe the operational limits of individual components in the power system, such as generators, reactive power compensators, transmission lines, and tap changers.

Constraints for generator

The active and reactive power generation, as well as the bus voltage magnitude of all generators in the power system, must conform to specified maximum and minimum limits, which are defined as follows:

$$P_{Gi}^{min} \leq P_{Gi} \leq P_{Gi}^{max} \qquad \text{For } i = 1,\ldots\ldots, NG \qquad (8)$$

$$V_{Gi}^{min} \leq V_{Gi} \leq V_{Gi}^{max} \qquad \text{For } i = 1, \ldots\ldots\ldots, NG \qquad (9)$$

$$Q_{Gi}^{min} \leq Q_{Gi} \leq Q_{Gi}^{max} \qquad \text{For } i = 1,\ldots\ldots, NG \qquad (10)$$

Constraints for transformers

The boundaries of the highest and lowest setting of the transformer tap changers are described as follows:

$$T_i^{min} \leq T_i \leq T_i^{max} \qquad \text{For } i = 1, \ldots\ldots\ldots, NT \qquad (11)$$

Constraints for shunt capacitors

The upper and lower margins of the reactive power from the shunt capacitor banks are given as follow:

$$Q_{Ci}^{min} \leq Q_{Ci} \leq Q_{Ci}^{max} \qquad \text{For } i = 1, \ldots\ldots\ldots, NC \qquad (12)$$

Constraints for load voltage

The voltage magnitude at all load buses should be kept inside the allowable boundaries as follow:

$$V_{Li}^{min} \leq V_{Li} \leq V_{Li}^{max} \qquad \text{For } i = 1,\ldots\ldots, NL \tag{13}$$

Security constraints

To ensure a secure power supply and prevent transmission lines from being overloaded, it is necessary to limit the maximum allowable apparent power flow for each section as follows:

$$S_{TLi} \leq S_{TLi}^{max} \qquad \text{For } i = 1,\ldots\ldots, NTL \tag{14}$$

3. Methodology

This section outlines the steps involved in the hybrid ARO-GBO technique. The algorithm proposed for this method is the ARO-GBO algorithm.

a. Artificial Rabbits Optimization (ARO)

The ARO technique imitates the behavior of real rabbits, including their foraging and hiding strategies, and their energy reserves that facilitate switching between these strategies [34].

1) Detour foraging

The algorithm exhibits a detour foraging behavior that involves updating the position of each search individual towards a random member of the swarm. This behavior introduces perturbations that aid in exploration. The mathematical model developed to describe the detour foraging behavior of rabbits is given below.

$$v_i(t+1) = x_j(t) + R \times \left(x_i(t) - x_j(t)\right) + round\left(0.5 \times (0.05 + r_1)\right) \times n_1, \;\; i,j = 1, \ldots, j \neq i \tag{15.1}$$

$$R = L \times c \tag{15.2}$$

$$L = (e - e^{\left(\frac{t-1}{T}\right)^2}) \times \sin(2\pi r_2) \tag{15.3}$$

$$c(k) = \begin{cases} 1 & if\ k == g(l) \\ 0 & else \end{cases} \; k = 1, \ldots, d \; and \; l = 1, \ldots, [r_3, d] \tag{15.4}$$

$$g = randperm(d), n_1 \sim N(0,1) \tag{15.5}$$

2) Random hiding

The following equation is formulated based on the behavior of rabbits, which often dig holes near their nest as a means of hiding from predators.

$$b_{i,j}(t) = x_i(t) + H.g.x_i(t), i = 1, \ldots., n \; and \; j = 1, \ldots., d \tag{16.1}$$

$$H = \frac{T - t + 1}{T}.r_4, n_2 \sim N(0,1) \tag{16.2}$$

$$g(k) = \begin{cases} 1 & if \; k == j \\ 0 & else \end{cases} \; k = 1, \ldots., d \tag{16.3}$$

To survive, rabbits need to search for a safe place to hide. Therefore, they tend to randomly choose a hole from their available variants to avoid getting caught. This random hiding behavior can be expressed mathematically as follows:

$$v_i(t+1) = x_i(t) + R \times \left(r_4 \times b_{ir}(t) - x_i(t)\right) \;\; i = 1, \ldots., n \tag{17.1}$$

$$g(k) = \begin{cases} 1 & if \; k == [r_5 \times d] \\ 0 & else \end{cases} \; k = 1, \ldots., d \tag{17.2}$$

$$b_{i,r}(t) = x_i(t) + H.g.x_i(t) \tag{17.3}$$

After one of both detour foraging and random hiding is attained, the location update of the i[th] rabbit is presented as:

$$x_i(t+1) = \begin{cases} x_i(t) & f(x_i(t) \leq f(v_i(t+1)) \\ v_i(t+1) & f(x_i(t) > f(v_i(t+1)) \end{cases} \tag{18}$$

3) Energy shrink

The algorithm incorporates an energy factor to represent the transition from exploration to exploitation. The energy factor can be defined as follows:

$$A(t) = 4(1 - \frac{t}{T}) \ln \frac{1}{r} \tag{19}$$

b. Gradient Based Optimizer (GBO)

The GBO [37] combines population-based and gradient-based methods by utilizing Newton's method. This involves exploring the search domain with a set of vectors and two essential operators: the Gradient Search Rule (GSR) and Local Escaping Operators (LEO).

1) GRADIENT SEARCH RULE (GSR) PROCESS

The GBO technique uses the Gradient Search Rule (GSR) that follows a gradient-based method to enhance exploration and speed up the convergence rate. As a result, the new location can be expressed as follows [41]:

$$X_{n+1} = X_n - \frac{2\Delta x \times f(X_n)}{f(X_n + \Delta x) - f(X_n - \Delta x)} \tag{20}$$

Equation (20) will be modified to incorporate the population-based search theory, which is expressed in Equation (21).

$$GSR = randn \times \frac{2\Delta x\, X_n}{(x_{worst} - x_{best} + \varepsilon)} \tag{21}$$

where $randn$ is a random number with a normal distribution, x_{worst}, x_{best} represent the worst and best values of the solution achieved through the optimization procedure, ε is a small number within the interval [0, 0.1], and Δx is the change in position in each iteration. From the previous equations., the GSR can be calculated as follows:

$$GSR = randn \times \rho_1 \times \frac{2\Delta x\, X_n}{(x_{worst} - x_{best} + \varepsilon)} \tag{22}$$

where ρ_1 refers to the randomly produced parameter and it is defined from the next equation:

$$\rho_1 = (2 \times\ rand \times \alpha) - \alpha \tag{23}$$

$$\alpha = \left|\beta\ \sin\left(\frac{3\pi}{2} + \sin\left(\beta\frac{3\pi}{2}\right)\right)\right| \tag{24}$$

$$\beta = \beta_{min} + (\beta_{min} - \beta_{min})\left(1 - \left(\frac{m}{M}\right)^3\right)^2 \tag{25}$$

where α is a sine function for the transference from exploration to exploitation, β_{min} and β_{max} represent constant values 0.2 and 1.2, respectively, m denotes the current number of iterations, and M refers to the total number of iterations. The change Δx between the best solution x_{best} and a randomly selected location x_{r1}^m can be given by [42]:

$$\Delta x = rand(1{:}N) \times |step| \tag{26}$$

$$step = \frac{(x_{best} - x_{r1}^m) + \delta}{2} \tag{26-1}$$

$$\delta = 2 \times rand \times (\left|\frac{x_{r1}^m + x_{r2}^m + x_{r3}^m + x_{r4}^m}{4}\right| - x_n^m) \tag{26-2}$$

where $rand(1:N)$ is a random vector with N dimensions, $r1,\ r2,\ r3,$ and $r4$ ($r1 \neq r2 \neq r3 \neq r4 \neq n$) represent diverse integers chosen by random from [1, N], $step$ is a step size. The new position X_{n+1} can be updated based on the GSR as follows:

$$X_{n+1} = X_n - GSR \tag{27}$$

The direction of movement (DM) is added for better exploitation of the nearby area of X_n which is calculated as follows:

$$DM = rand \times \rho_2 \times (x_{best} - x_n) \tag{28}$$

$$\rho_2 = (2 \times\ rand \times \alpha) - \alpha \tag{28-1}$$

Accordingly, the new position $X1_n^m$ is computed while taken the GSR and DM into consideration as below:

$$X1_n^m = x_n^m - \mathrm{GSR} + \mathrm{DM} \tag{29}$$

$$X1_n^m = x_n^m - randn \times \rho_1 \times \frac{2\Delta x \times x_n^m}{(x_{\mathrm{worst}} - x_{best} + \varepsilon)} + rand \times \rho_2 \times (x_{best} - x_n^m) \tag{30}$$

The GBO employed another position to increase the local search by putting x_{best} rather than x_n^m. Hence, the new position ($X2_n^m$) is represented as below:

$$X2_n^m = x_{\mathrm{best}} - randn \times \rho_1 \times \frac{2\Delta x \times x_n^m}{(yp_n^m - yq_n^m + \varepsilon)} + rand \times \rho_2 \times (x_{r1}^m - x_{r2}^m) \tag{31}$$

where,

$$yp_n = rand \times (\frac{[z_{n+1} + x_n]}{2} + rand \times \Delta x) \tag{32}$$

$$yq_n = rand \times (\frac{[z_{n+1} + x_n]}{2} - rand \times \Delta x) \tag{33}$$

According to the positions $X1_n^m, X2_n^m$, and the current position (X_n^m), the new position at the next iteration (x_n^{m+1}) is defined from the following equation:

$$x_n^{m+1} = r_a \times (r_b \times X1_n^m + (1 - r_b) \times X2_n^m) + (1 - r_a) \times X3_n^m \tag{34}$$

$$X3_n^m = X_n^m - \rho_1 \times (X2_n^m - X1_n^m) \tag{34-1}$$

1) Local escaping operator (LEO)

The Local Escaping Operator (LEO) is utilized to enhance the performance of the GBO algorithm and escape local optima when dealing with complex problems. The LEO generates a promising solution (X_{LEO}^m) by utilizing various solutions, including x_{best}, solutions $X1_n^m$, and $X2_n^m$, two random solutions x_{r1}^m andx_{r2}^m, and a newly generated random solution (x_k^m). The solution X_{LEO}^m is expressed as:

$if\ rand < pr$

$if\ rand < 0.5$

$$X_{LEO}^{m} = X_n^{m+1} + f_1 \times (u_1 \times x_{\text{best}} - u_2 \times x_k^m) + f_2 \times \rho_1 \times (u_3 \times (X2_n^m - X1_n^m) + u_2 \times (x_{r1}^m - x_{r2}^m))/2$$

$$X_n^{m+1} = X_{LEO}^m$$

Else

$$X_{LEO}^{m} = x_{\text{best}} + f_1 \times (u_1 \times x_{\text{best}} - u_2 \times x_k^m) + f_2 \times \rho_1 \times (u_3 \times (X2_n^m - X1_n^m) + u_2 \times (x_{r1}^m - x_{r2}^m))/2 \quad (35)$$

$$X_n^{m+1} = X_{LEO}^m$$

End

End

where f_1 is a uniform distributed random number in the range of [-1,1], f_2 denotes a random number from a normal distribution with a mean of 0 and a standard deviation of 1. Additionally, pr denotes the probability, and u_1, u_2, and u_3 represent random values generated as below [41]:

$$u_1 = \begin{cases} 2 \times rand & if\ \mu_1 < 0.5 \\ 1 & otherwise \end{cases} \quad (36)$$

$$u_2 = \begin{cases} rand & if\ \mu_1 < 0.5 \\ 1 & otherwise \end{cases} \quad (37)$$

$$u_3 = \begin{cases} rand & if\ \mu_1 < 0.5 \\ 1 & otherwise \end{cases} \quad (38)$$

where $rand$ refers to a random number in the range of [0, 1], and μ_1 is a number in the range of [0, 1]. The previous equations can be defined as below:

$$u_1 = L_1 \times 2 \times rand + (1 - L_1) \quad (39)$$

$$u_2 = L_1 \times rand + (1 - L_1) \quad (40)$$

$$u_3 = L_1 \times rand + (1 - L_1) \quad (41)$$

where L_1 denotes a binary parameter with a value of 0 or 1. If parameter μ_1<0.5, the value of L_1 = 1, otherwise, L_1= 0. The solution x_k^m is created as below:

$$x_k^m = \begin{cases} x_{rand} & if\ \mu_2 < 0.5 \\ x_p^m & otherwise \end{cases} \quad (42)$$

$$x_{rand} = X_{min} + rand(0,1) \times (X_{max} - X_{min}) \quad (43)$$

where x_{rand} refers to a random generated solution, x_p^m is a randomly selected solution of the population ($p \in [1, 2, \dots, N]$), and μ_2 denotes a random number in the range of [0, 1]. Eq. (42) is simplified as:

$$x_k^m = L_2 \times x_p^m + (1 - L_2) \times x_{rand} \quad (44)$$

where L_2 refers to a binary parameter with a value of 0 or 1. If μ_2<0.5, the value of L_2=1, otherwise, L_2=0. The flowchart of hybrid ARO-GBO algorithm is shown in Figure 1.

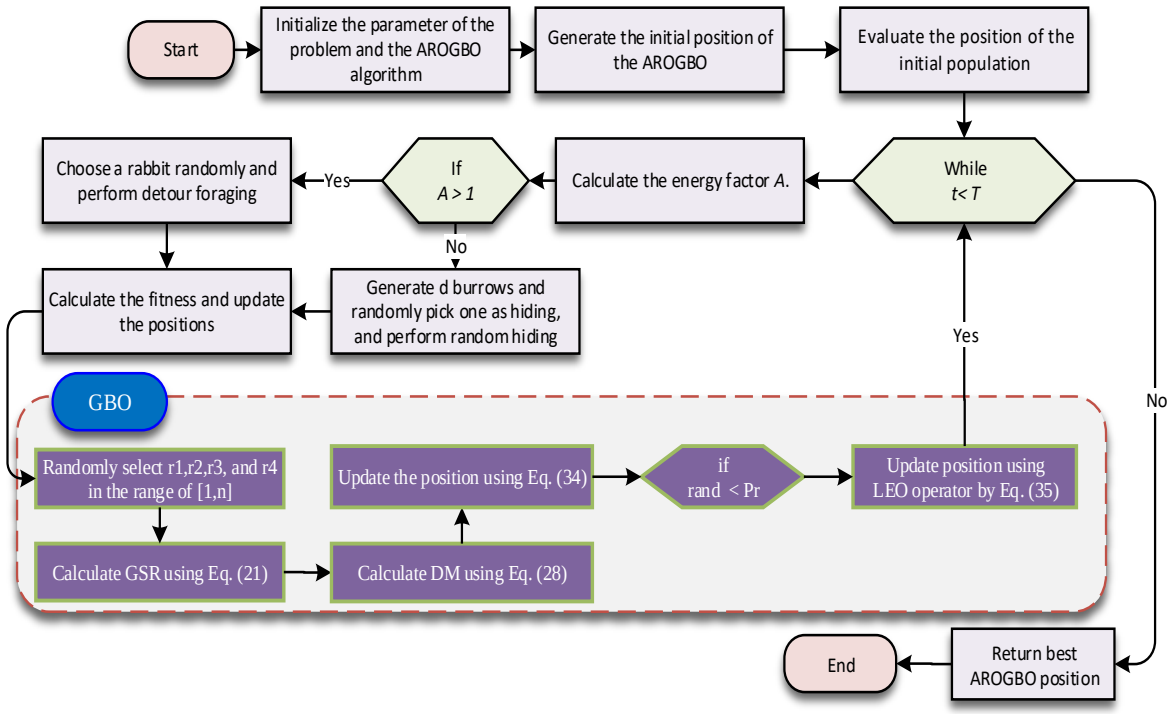

Figure.1. Flowchart of hybrid AROGBO algorithm.

4. Results and discussion

a. Benchmark functions

In this section, we demonstrate the effectiveness of the hybrid AROGBO technique by assessing its performance on seven benchmark functions. The mathematical expressions for these test functions can be found in [64]. Our benchmark experiments were conducted using MATLAB (R2016a) on a computer equipped with an Intel(R) Core i5-4210U CPU operating at 2.40 GHz and 8GB of RAM. To evaluate and compare the performance of the AROGBO technique, this study employs seven well-established benchmark test functions. All the metaheuristic methods discussed in this paper adhere to a consistent maximum iteration limit of 200 iterations, along with a uniform population size of 50.

In this section, we conduct a comparative analysis of the AROGBO technique against four recently proposed techniques: the northern goshawk optimization algorithm (NGO) [65], Pelican optimization algorithm (POA) [66], GBO, and ARO algorithms. The assessment of solution quality is based on mean values and standard deviations. Lower mean values and standard deviations indicate robust global optimization capabilities and greater stability. The statistical results derived from applying the AROGBO algorithm and four well-known algorithms to solve seven benchmark functions are presented in Table 1.

As shown in Table 1, the AROGBO technique consistently outperforms other evaluated methods across the majority of benchmark functions in terms of the mean value. The data clearly indicates that the AROGBO algorithm consistently achieves more favorable solutions compared to recently proposed techniques for solving various benchmark functions. Furthermore, the AROGBO approach surpasses NGO, POA, GBO, and ARO techniques in addressing benchmark functions. This analysis underscores the efficiency of the AROGBO algorithm. The tied rank method, a statistical approach used to compare the performance of multiple techniques in the presence of ties in the performance metric, reveals that the AROGBO technique exhibits superior performance across the majority of the seven benchmark optimization problems, as evidenced by its ranking order. GBO and POA algorithms secure the second and third positions, both demonstrating robust efficacy. This collective evidence establishes the AROGBO technique as a highly effective algorithm for successfully identifying optimal solutions within this category of problems.

Table 1 the statistical results of seven benchmark functions by the AROGBO algorithm and other well-known techniques.

Function		AROGBO	GBO	ARO	NGO	POA
F1	Best	1.7E-248	9.06E-52	1.59E-26	5.01E-34	1.18E-45
	Average	1.6E-231	4.1E-46	1.07E-21	7.16E-33	1.62E-37
	Median	1.6E-237	1.73E-49	4.68E-23	4.24E-33	1.86E-41
	Worst	1.5E-230	4.79E-45	7.08E-21	3.02E-32	3.09E-36
	std	0	1.27E-45	2.18E-21	8.77E-33	6.9E-37
	Rank	1	2	5	4	3
F2	Best	1.2E-124	2.03E-28	1.34E-14	6.6E-18	3.79E-23
	Average	1.3E-113	1.95E-24	1.15E-12	1.65E-17	3.15E-20
	Median	9.5E-118	1.77E-25	1.22E-13	1.58E-17	5.04E-21
	Worst	1.3E-112	1.95E-23	1.78E-11	3.85E-17	1.67E-19
	std	4E-113	4.64E-24	3.94E-12	7.66E-18	4.9E-20
	Rank	1	2	5	4	3
F3	Best	1.3E-247	3.42E-42	4.28E-21	1.04E-08	1.74E-43
	Average	3.2E-221	2.56E-38	5.08E-15	1.19E-06	8.76E-39
	Median	2.3E-236	5.51E-40	6.99E-17	1.85E-07	3.91E-41
	Worst	3.2E-220	2.05E-37	6.41E-14	1.35E-05	1.19E-37
	std	0	5.68E-38	1.51E-14	3.02E-06	2.76E-38
	Rank	1	3	4	5	2
F4	Best	7.1E-125	1.54E-24	8.35E-13	1.39E-14	2.06E-24
	Average	6.6E-114	8.59E-22	2.6E-09	3.71E-14	5.73E-20
	Median	7.7E-119	1.22E-22	7.79E-10	3.34E-14	4.04E-21
	Worst	6.4E-113	1.08E-20	2.28E-08	7.08E-14	4.68E-19
	std	2E-113	2.47E-21	5.09E-09	1.77E-14	1.29E-19
	Rank	1	2	5	4	3
F5	Best	24.41348	24.25387	0.048127	26.83203	27.59768

	Average	24.89583	25.13063	2.57084	27.31122	28.57786
	Median	24.83941	25.117	1.069097	27.2574	28.75691
	Worst	25.98472	26.10917	16.26736	27.8186	28.8694
	std	0.442207	0.565603	3.783419	0.253381	0.376116
	Rank	2	3	1	4	5
F6	Best	3.46E-05	0.00018	0.009568	0.189623	2.287489
	Average	0.000218	0.00108	0.044563	0.337336	3.220579
	Median	0.000171	0.000875	0.039666	0.314621	3.076281
	Worst	0.000533	0.002836	0.098375	0.557148	4.6641
	std	0.000183	0.000702	0.026373	0.115208	0.548631
	Rank	1	2	3	4	5
F7	Best	1.06E-05	0.000111	3.22E-05	0.000308	1.74E-05
	Average	0.000216	0.001192	0.001407	0.001318	0.000404
	Median	0.000179	0.000985	0.00115	0.001333	0.000328
	Worst	0.000509	0.004017	0.003564	0.003044	0.001649
	std	0.000187	0.001008	0.001071	0.000676	0.000361
	Rank	1	3	5	4	2
Average Rank		1.142857	2.428571	4	4.142857	3.285714
Final ranking		1	2	4	5	3

Furthermore, the convergence curves unmistakably emphasize the consistent superiority of the AROGBO technique when compared to other methods across the majority of benchmark functions. This underscores its robustness and adaptability in addressing a diverse spectrum of optimization problems. The exceptional performance of the AROGBO technique can be attributed to its effective amalgamation of the ARO algorithm and GBO algorithm. This combination empowers it to skillfully navigate the search space, exploit promising regions, and achieve faster convergence with superior solutions.

Moreover, the convergence curves, illustrated in Figure 2, not only affirm the rapid convergence of the AROGBO technique but also highlight its ability to maintain stable and reliable performance throughout the optimization process. This is a crucial characteristic for an optimization algorithm, ensuring that it consistently identifies optimal solutions without being trapped in local minima. Additionally, the experimental findings indicate that the AROGBO technique exhibits resilience to variations in optimization parameters, such as population size and crossover probability. This resilience implies that the AROGBO algorithm can be seamlessly applied to diverse problem domains without the need for extensive parameter fine-tuning.

In conclusion, these findings firmly establish the AROGBO technique as a powerful and versatile optimization method capable of efficiently attaining optimal solutions for a broad spectrum of real-world optimization challenges. The algorithm's swift convergence, unwavering performance, and

parameter robustness position the AROGBO technique as an attractive choice for both practitioners and researchers.

The numerical data is represented visually using box plots, which depict the distribution of optimal values obtained from multiple runs for each algorithm. Figure 3 showcases these box plots for seven benchmark functions, based on data collected from 30 individual iterations. Box plots are highly effective in illustrating data distribution and highlighting data consistency. Upon examining Figure 3, it becomes evident that the box plots for the AROGBO technique exhibit narrower spreads and consistently rank among the lowest values for most functions. These visual representations serve as powerful tools for evaluating the performance of the nonlinear system, providing a clear comparison between different techniques. The results unequivocally highlight the superior performance of the AROGBO method.

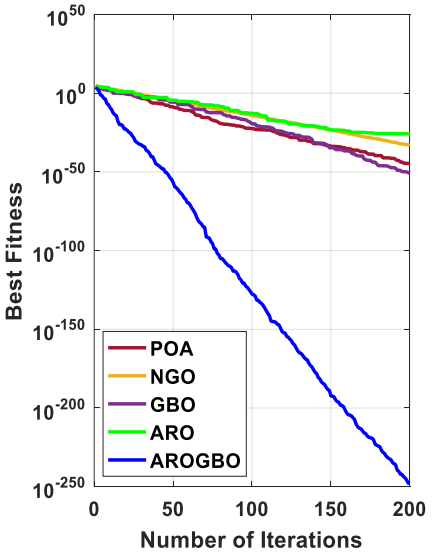

F1

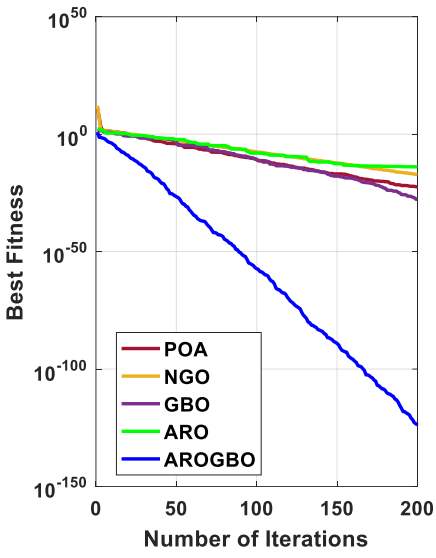

F2

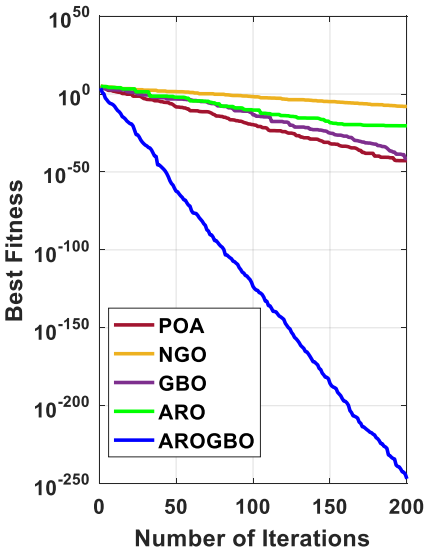

F3

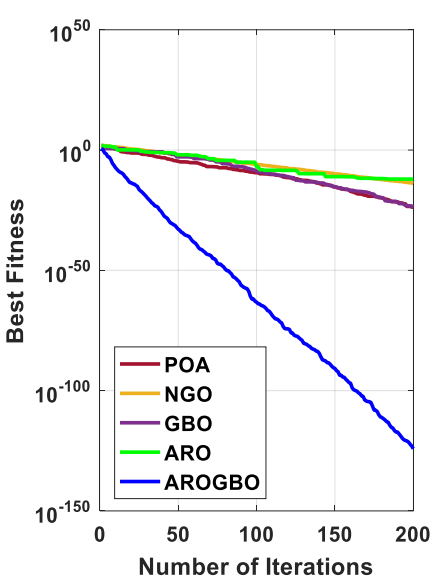

F4

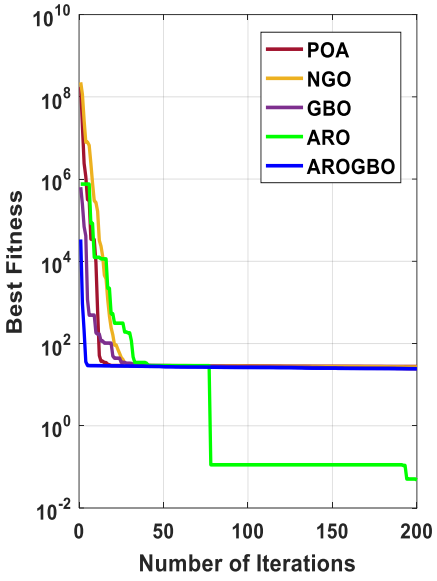

F5

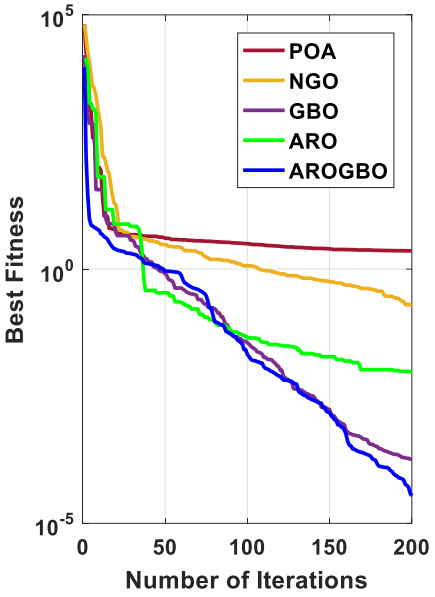

F6

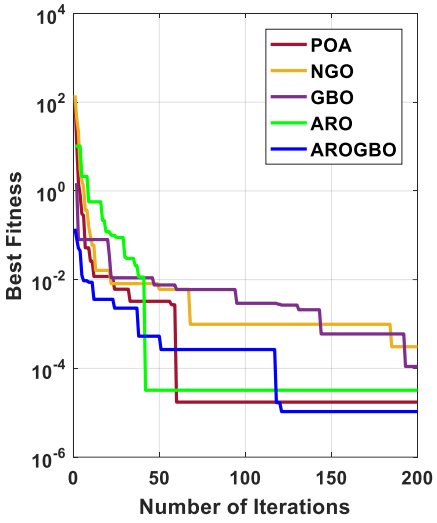

F7

Figure 2. The convergence characteristics of the studied techniques for the benchmark functions.

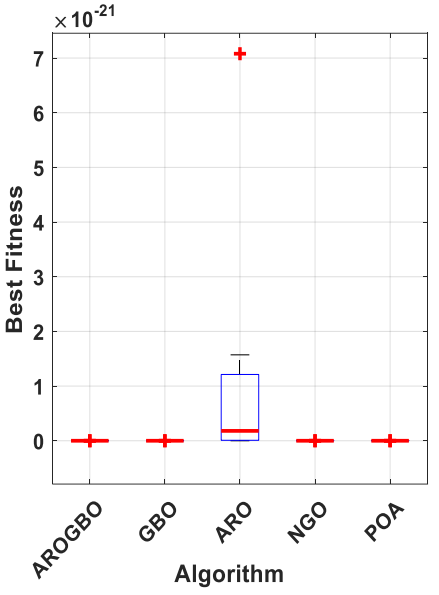

F1

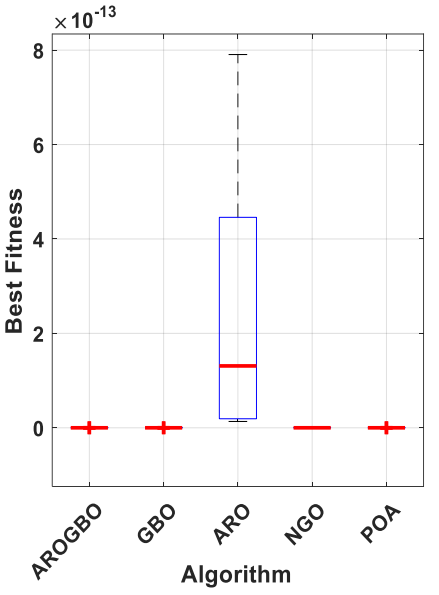

F2

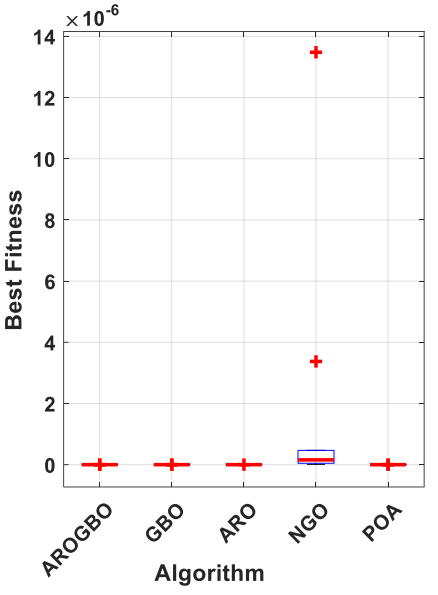

F3

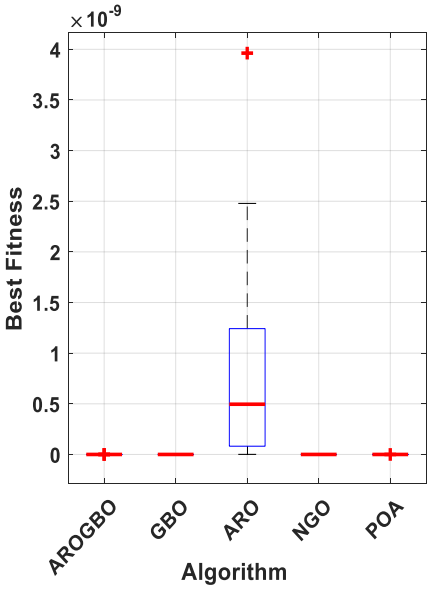

F4

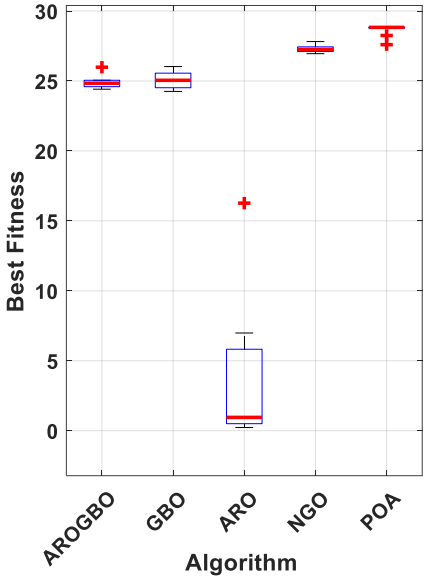

F5

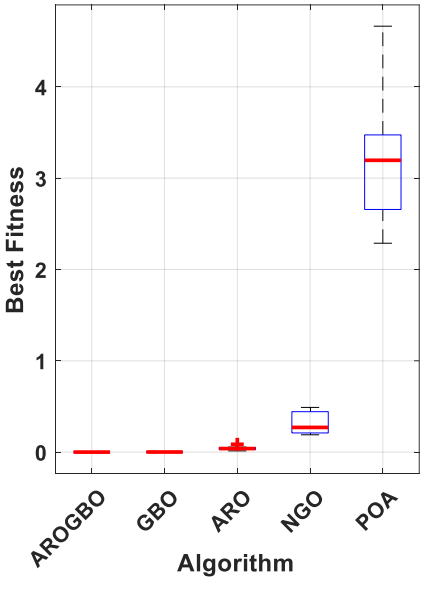

F6

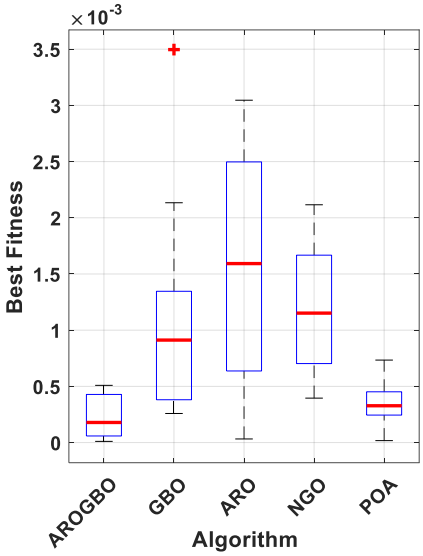

F7

Figure 3. Boxplots of the studied techniques for the benchmark functions.

1) Wilcoxon's rank test results

In this subsection, we delve into a more detailed statistical analysis to evaluate the variances between AROGBO and other techniques using the Wilcoxon rank-sum test (WRST), a paired assessment method employed to discern significant differences between the two techniques. The outcomes of these tests, conducted at a significance level of α=0.05, are elucidated in Table 2. Within the table, symbols like "+/=/-" indicate whether AROGBO performs better, similarly, or worse than the compared technique. Furthermore, the table furnishes statistical insights into AROGBO's performance across different dimensions and functions, elucidating whether it outperforms, performs similarly, or lags behind the comparison algorithm.

It is noteworthy that AROGBO exhibits superior statistical performance in F1-F7 with Dim=30 when compared to other techniques, confirming its substantial dominance across most functions. Consequently, we can confidently assert that the proposed AROGBO technique demonstrates the best overall performance when compared to other methods.

Table 2 Statistical results of the Wilcoxon rank-sum test.

AROGBO vs	ARO		GBO		NGO		POA	
Function	P	winner	P	winner	P	winner	P	winner
F1	1.83E-04	+	1.83E-04	+	1.83E-04	+	1.83E-04	+
F2	1.83E-04	+	1.83E-04	+	1.83E-04	+	1.83E-04	+
F3	1.83E-04	+	1.83E-04	+	1.83E-04	+	1.83E-04	+

F4	1.83E-04	+	1.83E-04	+	1.83E-04	+	1.83E-04	+
F5	1.83E-04	-	7.34E-01	=	1.83E-04	+	1.83E-04	+
F6	1.83E-04	+	1.83E-04	+	1.83E-04	+	1.83E-04	+
F7	1.71E-03	+	3.61E-03	+	4.40E-04	+	1.62E-01	=
WRST (+/=/-)	6/0/1		6/1/0		7/0/0		6/1/0	

2) Friedman's rank test results

Table 3 displays the statistical outcomes derived from Friedman tests conducted on seven benchmark functions utilizing the scrutinized algorithms. In this assessment, a lower ranking value signifies a more superior algorithm performance. The results unveil a clear ranking order among the five techniques, namely: AROGBO, ARO, GBO, NGO, and POA. This established ranking order provides valuable insights into the relative performance of these algorithms across the benchmark functions, with AROGBO emerging as the top-performing technique, followed by GBO, POA, ARO, and NGO in descending order. These findings provide a comprehensive perspective on how the algorithms compare to each other across various test functions.

Table 3 Friedman test for the five algorithms.

Function	AROGBO	ARO	GBO	NGO	POA
F1	1	5	2	4	3
F2	1	5	2	4	3
F3	1	4	2.7	5	2.3
F4	1	5	2.1	4	2.9
F5	2.5	1	2.5	4	5
F6	1	3	2	4	5
F7	1.6	3.7	3.7	3.9	2.1
Mean ranks	1.3	3.814286	2.428571	4.128571	3.328571

b. The study case results

To tackle the optimization problem of reactive power dispatch, the study utilized ARO, GBO, and a hybrid AROGBO optimization technique. The experiment included two standard test systems: IEEE 30-bus system, IEEE 57-bus system, and IEEE 118-bus system, and two different objective functions were used to validate the proposed algorithms. The first objective function aimed to minimize power losses in the distribution system, while the second one aimed to minimize the total voltage drop at all buses of the distribution network. To account for the stochastic nature of the metaheuristic algorithms, the algorithms were implemented 20 times, and parametric and non-parametric statistical analysis were conducted to confirm the accuracy and robustness of the proposed optimization techniques. The control parameters for all algorithms were set to a maximum iteration of 500 and a population size of 50. Table 4 provides a brief description of the standard systems (IEEE 30-bus, IEEE 57-bus, and IEEE 118-bus) and the findings of the base case without any optimization techniques applied.

The following subsections present the achievements of the optimization process for the four case studies. The results are extensively compared with recently proposed optimization methods such as PSO with time-varying acceleration coefficients (PSO-TVAC) [43], self-organizing PSO with TVAC (SPSO-TVAC) [43], stochastic weight trade-off PSO (SWT-PSO) [43], antlion optimization algorithm (ALO) [44], water cycle algorithm (WCA) [45], pseudo-gradient PSO (PG-PSO) [43], modified colliding bodies optimization algorithm (MCBOA) [46], specialized genetic algorithm (SGA) [47], backtracking search optimizer (BSO) [48], multi-objective GWO [49], PSO with an aging leader and challengers (ALC-PSO) [50], hybrid PSO and imperialist competitive algorithms (PSO-ICA) [51], multi-

objective ant lion optimization (MOALO) [52], Gaussian bare-bones WCA (GBWCA) [45], and opposition-based gravitational search algorithm (OGSA) [53].

Table 4. Characteristics of the standard IEEE systems.

Variable	IEEE 30 Bus test system	IEEE 57 Bus test system	IEEE 118 Bus test system
Bus number (NB)	30.0	57.0	118.0
Generators number (NG)	6.0	7.0	54
Transformers number (NT)	4.0	15.0	9.0
Capacitor bank number (NQ)	9.0	3.0	14.0
Line sections number (NE)	41.0	80.0	186.0
Control variables	19.0	27.0	77
Base value of Ploss (MW)	5.660	27.8637	132.8629
Base value of TVD (p.u)	0.58217	1.23358	1.4393

Case - 1

In this subsection, the results of using ARO, GBO, and the hybrid AROGBO optimization techniques to address the issue of reactive power dispatch in the IEEE 30-bus test system while minimizing the total power losses consumed in the system as the objective function are presented. Figure 4 shows a single-line representation of the proposed IEEE-30 bus test network. The three algorithms were implemented 20 times, and the obtained objective function values (min P_{loss}) were recorded. Figure 5 displays a graphical representation of the 20 values obtained from all methods, and Table 5 presents the statistical measurements of the results obtained for the three techniques.

The results of the parametric statistical study, including minimum, maximum, mean, and median, showed that the hybrid AROGBO algorithm outperformed the traditional ARO and GBO methods when addressing the optimization issue. The non-parametric statistical metrics, such as standard deviation (SD), relative error (RE), mean absolute error (MAE), and root mean square error (RMSE), demonstrated the stability and robustness of the developed hybrid AROGBO methodology. The superiority of the suggested AROGBO algorithm is also confirmed by the boxplot representation of the obtained results presented in Figure 6.

Furthermore, the convergence trends of the run that resulted in the minimum value of the objective function for the three algorithms are shown in Figure 7. It is evident that the developed AROGBO methodology achieved the minimum value of the objective function in fewer iterations compared to the other methods.

Table 6 presents the optimal values of generator voltage, transformer tap changer positions, and reactive power compensation achieved through the best run of the proposed algorithms out of the 20 runs. It is evident from Table 6 that the AROGBO method resulted in the optimal value of power losses in the system. Furthermore, the obtained results of the optimization process based on the three algorithms were utilized to calculate the bus voltage and reactive power generation values through the power flow program, which were recorded. Figure 8 displays the voltage magnitude values at all buses of the IEEE 30-bus system, which are within the predefined limits. The voltage profile obtained using the AROGBO method was superior to those of other algorithms. Figure 9 illustrates the reactive power generation values of the six generators of the IEEE 30-bus system as reported in Table 6. To further validate the results, the proposed AROGBO technique was compared with recent optimization techniques used for solving RPD in the IEEE 30-bus system and listed in Table 7. It can be observed that the AROGBO method resulted in the minimum value of the objective function compared to all the other algorithms in the comparison.

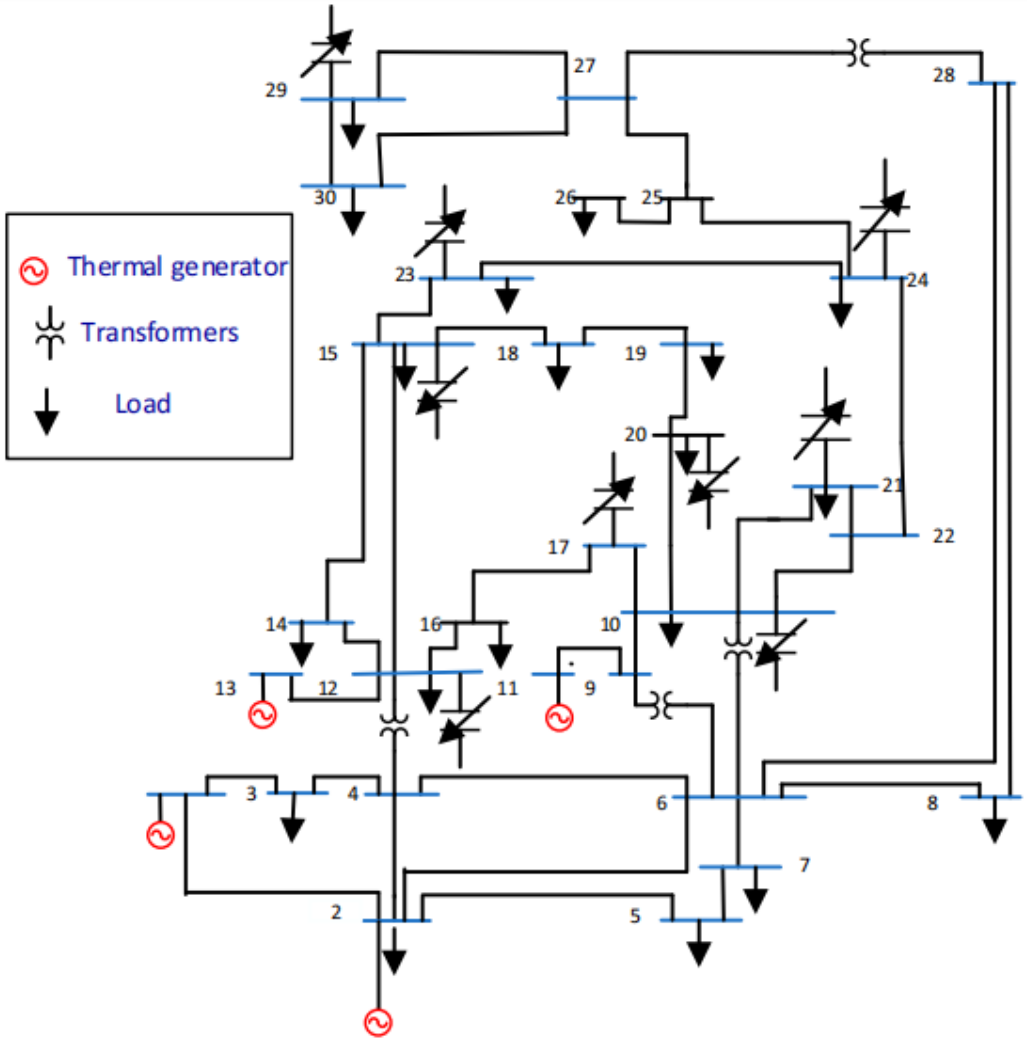

Figure 4. Single line representation of the IEEE 30-bus system.

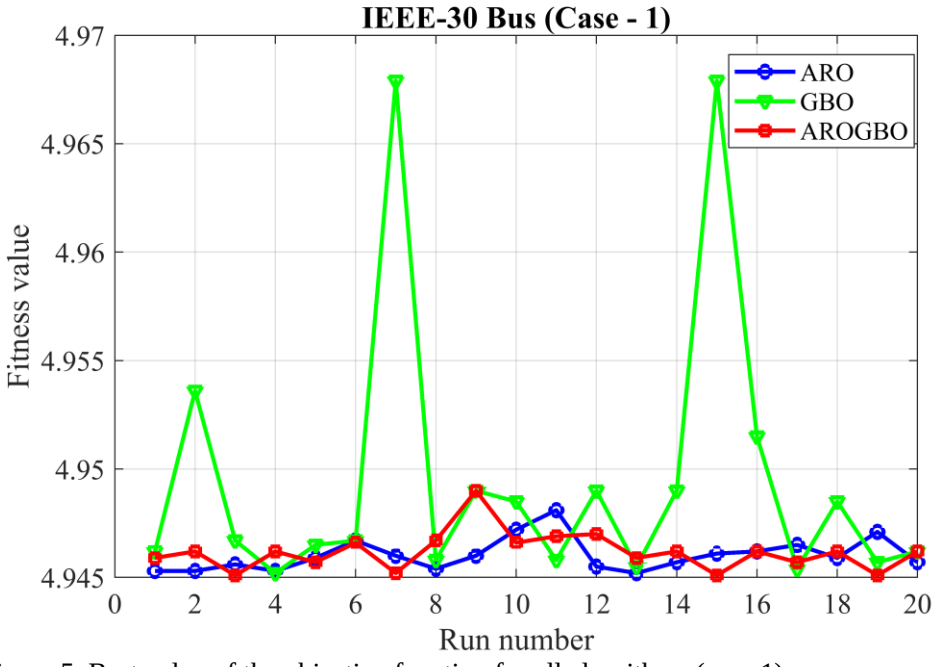

Figure 5. Best value of the objective function for all algorithms (case 1).

Table 5. Statistical results based on the 20 runs for all algorithms (case 1).

IEEE 30 Bus (Case-1)			
	ARO	**GBO**	**AROGBO**
Best	4.9452000	4.9452000	4.9451000
Worst	4.9481000	4.9679000	4.9490000
Mean	4.9460350	4.9495300	4.9461850
Median	4.9459000	4.9467000	4.9462000
SD	0.0007576	0.0066501	0.0008839
RE	0.0033770	0.0175119	0.0043882
MAE	0.0008350	0.0043300	0.0010850
RMSE	0.0011147	0.0077949	0.0013855

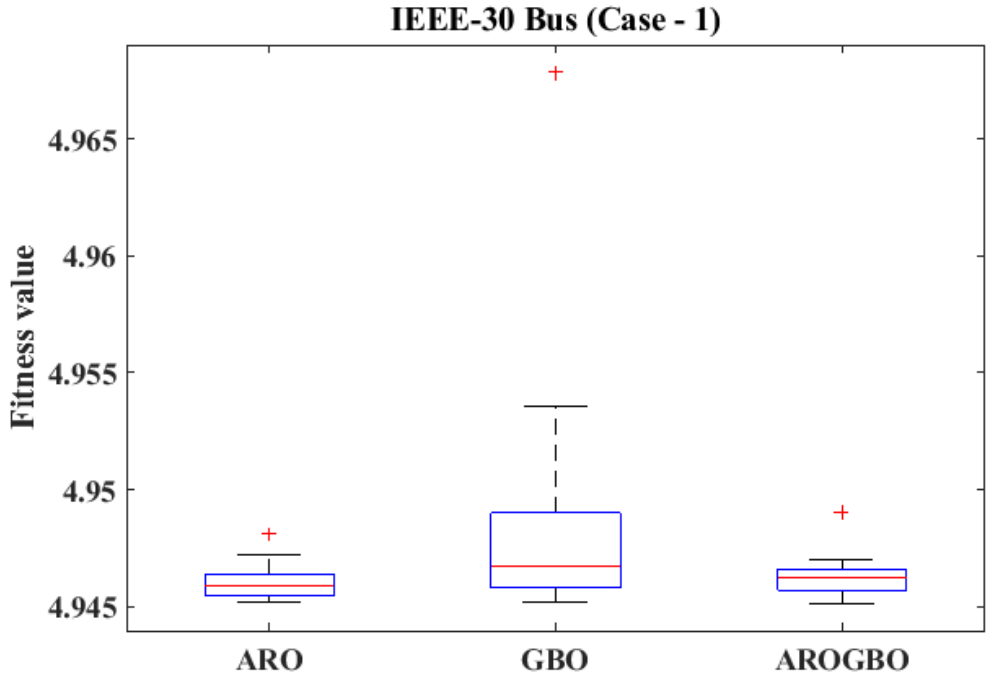

Figure 6. Boxplot representation for the results of the 20 runs from all techniques for case -1.

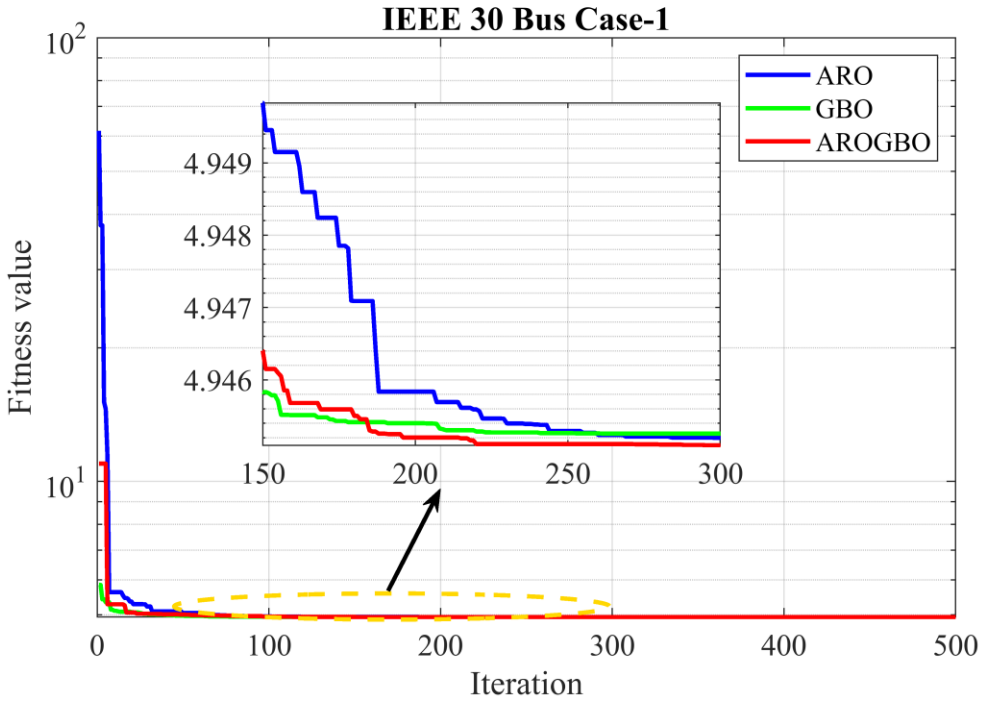

Figure 7. Convergence trends of all algorithms for case 1.

Table 6. Results of the optimization process for case -1.

Parameter	Case-1 (Min Losses)				
	Min.	Max.	ARO	GBO	AROGBO
Generator voltage (p.u.)					
V1	0.950	1.10	1.071589771	1.071779462	1.07184609
V2	0.950	1.10	1.062569698	1.06272039	1.062660176
V5	0.950	1.10	1.040230056	1.040621106	1.040234655
V8	0.950	1.10	1.040072305	1.040423149	1.040516195
V11	0.950	1.10	1.037932049	1.034373642	1.025468207
V13	0.950	1.10	1.059497196	1.058904726	1.05916275
Transformer Tap ratio (p.u.)					
T11	0.90	1.10	0.993265125	0.988444384	1.012753396
T12	0.90	1.10	0.938596537	0.947844365	0.91146225
T15	0.90	1.10	0.979353038	0.978007929	0.978510916
T36	0.90	1.10	0.986694381	0.987161433	0.987396578
Capacitor Bank (MVAr)					
Q10	0	5	2.227232185	3.280317677	3.588949402
Q12	0	5	0.144277927	0.222549486	0.226007841
Q15	0	5	2.37480135	2.093469617	3.655505729
Q17	0	5	4.174062917	3.019716053	3.878558782
Q20	0	5	3.680649374	4.218425351	1.502474996
Q21	0	5	0.959593681	4.125136051	1.686223593
Q23	0	5	1.817521144	4.441784265	2.365914452
Q24	0	5	1.864663061	1.423991794	3.261484316
Q29	0	5	4.46808624	4.661414433	0.700228303
Fitness value					

P_{losses} (MW)			4.945160379	4.945244011	4.945087807
Generator reactive power (MVAr)					
QG1	-29.8	59.6	-3.143190	-2.96104	-2.68766
QG2	-24	48	11.96442	11.8983	11.8386
QG5	-30	60	1.682433	1.93094	1.63766
QG8	-26.5	53	26.00022	26.6617	27.2576
QG11	-7.5	15	-5.335272	-7.20423	-7.18620
QG13	-7.8	15.5	7.439920	6.98706	7.18504

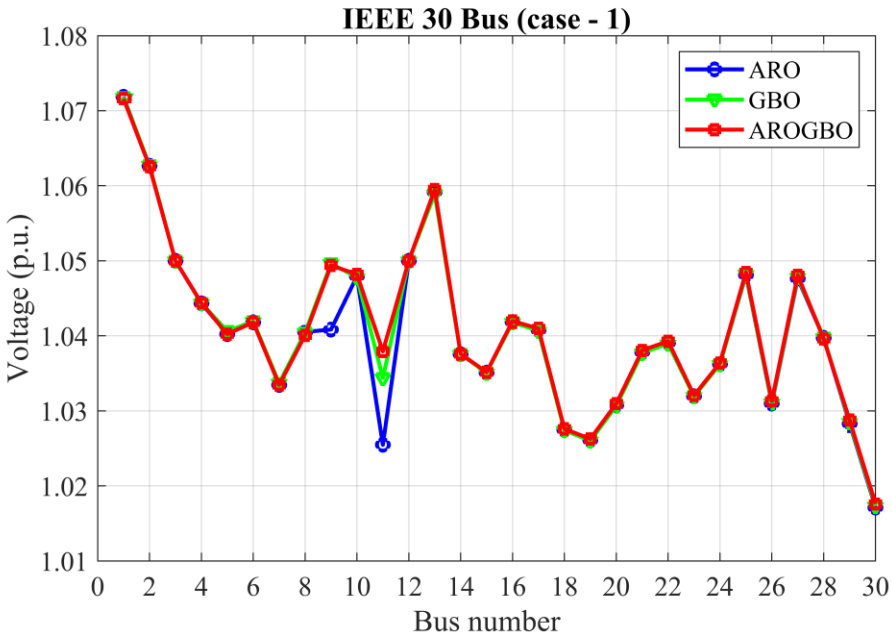

Figure 8. Voltage profile based on all techniques for case 1.

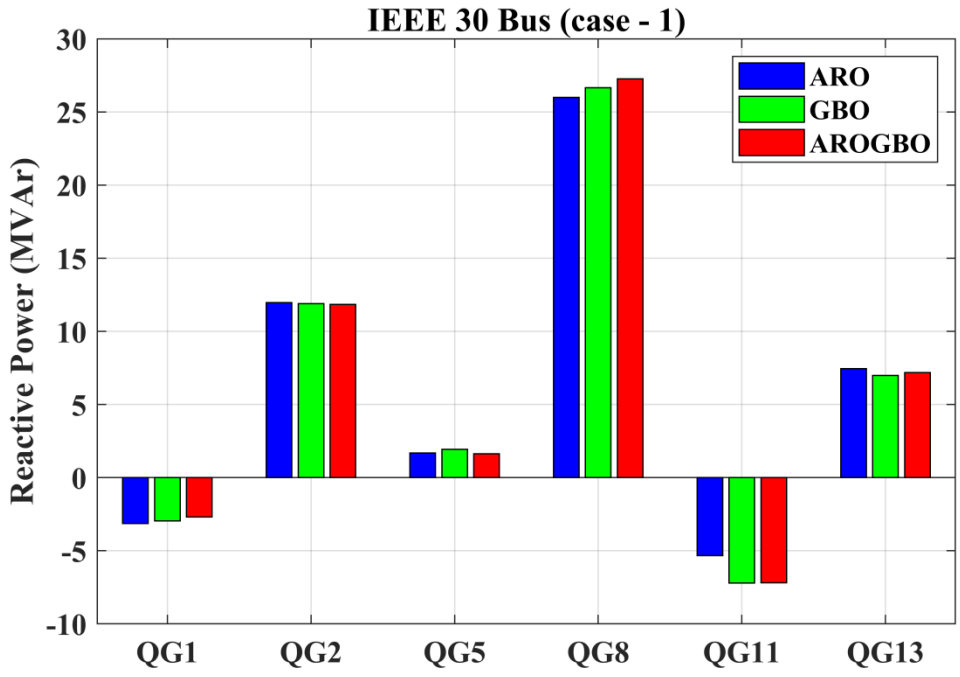

Figure 9. Reactive power generation at the generator buses based on all techniques for case 1.

Table 7. Comparison of the attainments of AROGBO algorithm with other algorithms for case 1.

Case -1		
Algorithm	Best	Average
SF-DE [24]	4.946	4.947
RSO [54]	5.133	-
SP-DE[24]	4.947	4.9667
EC-DE[24]	4.946	4.9476
GS [55]	5.101	-
SR-DE[24]	4.946	4.9481
ECHT-DE[24]	4.947	4.9499
ALC-PSO [29]	5.1861	-
EB [11]	4.963	-
QODE [12]	5.2953	-
PSOGWO [20]	5.09037	-
CKHA [18]	5.1163	-
GA [20]	5.0977	-
OGSA [29]	5.1676	-
PSO [20]	5.1041	-
ARO	4.945160379	4.9460350
GBO	4.945244011	4.9495300
AROGBO	4.945087807	4.9461850

Case - 2

In this subsection, the findings of the ARO, GBO, and hybrid AROGBO optimization techniques are presented for addressing the issue of RPD in the IEEE 30-bus test system, with the objective function of minimizing the TVD at all buses. Figure 10 presents a graphical representation of the 20 values of the objective function (min TVD) obtained from all three algorithms. The statistical analysis of the obtained results from the 20 runs for the three methods is shown in Table 8, indicating the accuracy and robustness of the hybrid AROGBO methodology. The effectiveness of the AROGBO algorithm is further confirmed by the boxplot representation in Figure 11. The convergence trends of the three algorithms are demonstrated in Figure 12, where it is evident that the AROGBO method converged in fewer iterations compared to the other methods. Table 9 shows the results of the optimization process for the best run within the 20 runs of the three algorithms. It is evident that the developed AROGBO method reached the lowest value of the total voltage deviations in the system.

Figure 13 displays the voltage magnitude at the 30 buses of the system, which indicates that the voltage profile based on the results of the AROGBO technique outperforms other algorithms. Additionally, the values of the reactive power generation from the six generators included in the IEEE 30-bus system are presented in graphical form in Figure 14, as reported in Table 9. To further validate the performance of the proposed hybrid AROGBO algorithm, the obtained results are compared with recent optimization techniques used for solving the

RPD in the IEEE 30-bus system, and the comparison is provided in Table 10, where it is observed that the proposed AROGBO achieved the minimum value of the objective function compared to other algorithms.

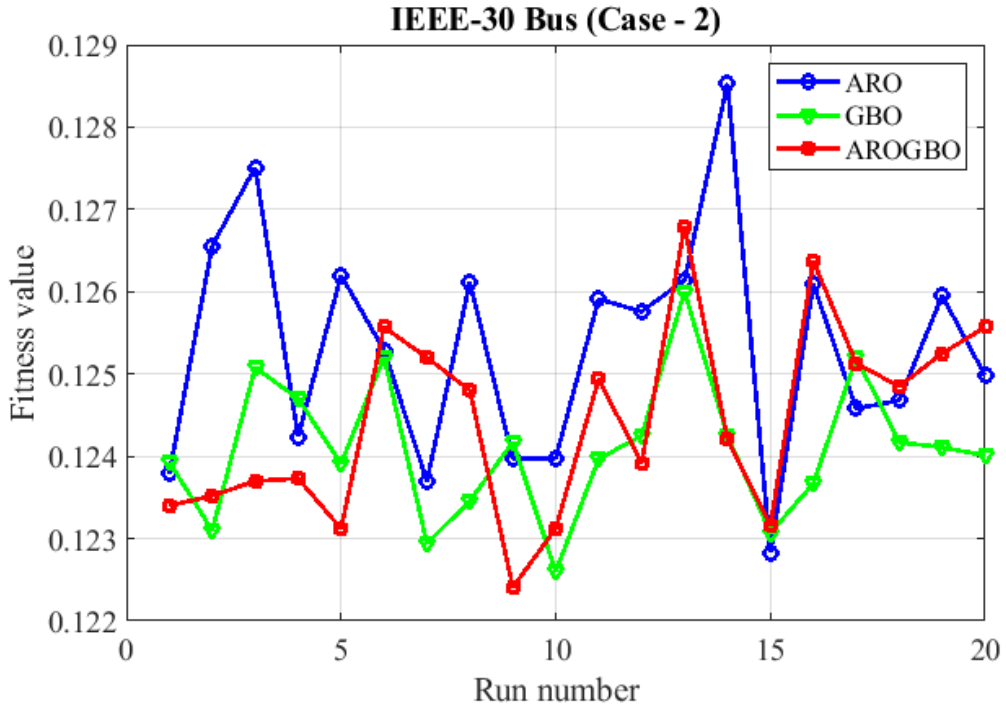

Figure 10. Best value of the objective function for all algorithms (case 2).

Table 8. Statistical results based on the 20 runs for all algorithms (case 2).

IEEE 30 Bus (Case-2)			
	ARO	**GBO**	**AROGBO**
Best	0.1228300	0.1226000	0.1224100
Worst	0.1285300	0.1260000	0.1267900
Mean	0.1253405	0.1240900	0.1244380
Median	0.1255250	0.1240600	0.1245050
SD	0.0014006	0.0008512	0.0011833
RE	0.4087764	0.2430669	0.3313455
MAE	0.0025105	0.0014900	0.0020280
RMSE	0.0028577	0.0017054	0.0023330

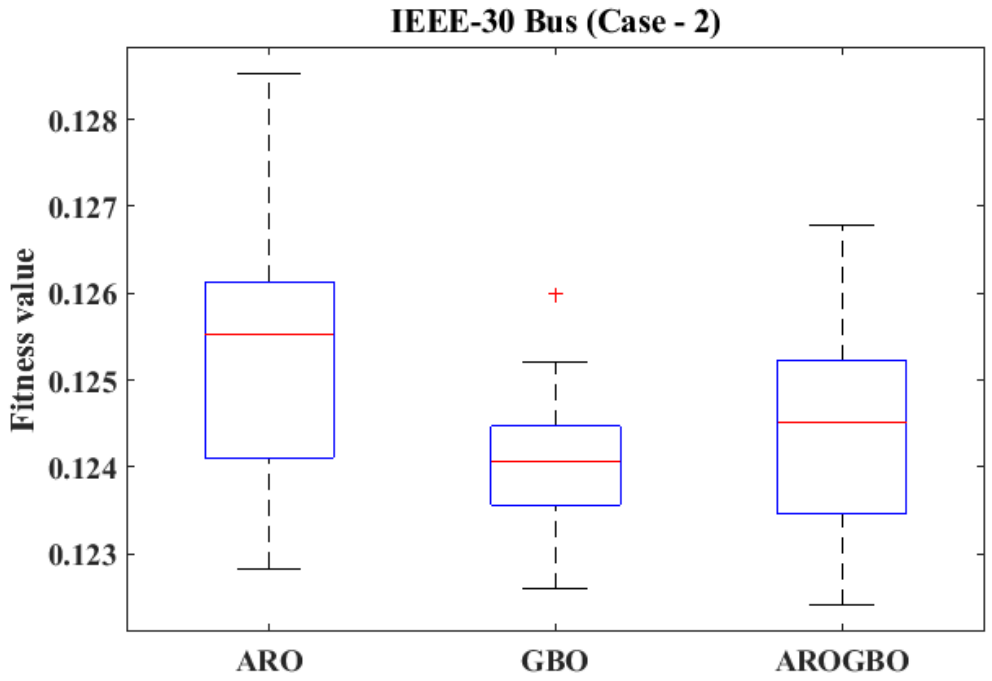

Figure 11. Boxplot representation for the results of the 20 runs from all techniques for case 2.

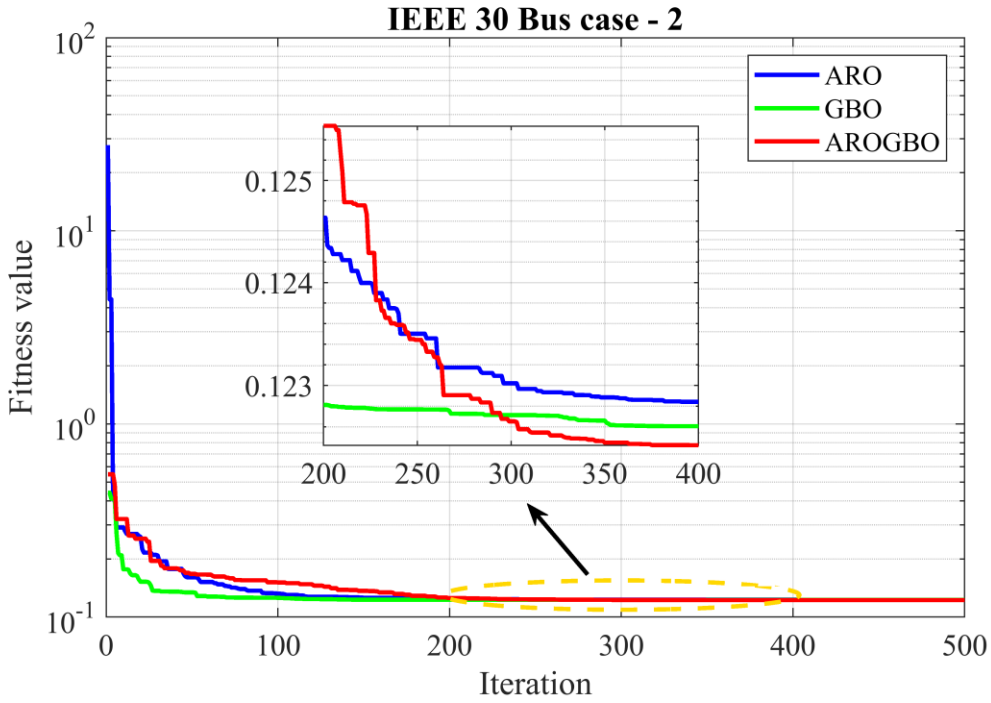

Figure 12. Convergence trends of all algorithms for case 2.

Table 9. Results of the optimization process for case -2.

	Case -2 (min VD)				
Parameter	Min.	Max.	ARO	GBO	AROGBO
Generator voltage (p.u.)					
V1	0.950	1.10	1.00850283	1.007501748	1.006197652
V2	0.950	1.10	1.007818046	1.008154279	1.007117126

V5	0.950	1.10	1.017893813	1.01706355	1.018125931
V8	0.950	1.10	1.004866212	1.005859828	1.004461959
V11	0.950	1.10	0.988244066	0.992256952	0.988550465
V13	0.950	1.10	1.021775804	1.020112478	1.02564065
Transformer Tap ratio (p.u.)					
T11	0.9	1.1	1.01746853	1.02197278	1.01880421
T12	0.9	1.1	0.91348107	0.91161506	0.91046131
T15	0.9	1.1	0.96572466	0.96303224	0.97201001
T36	0.9	1.1	0.96977962	0.97072174	0.96838166
Capacitor Bank (MVAr)					
Q10	0	5	3.49369118	2.58766183	4.54105603
Q12	0	5	3.10494898	3.47345008	1.66111576
Q15	0	5	4.30512657	4.08160621	0.72878144
Q17	0	5	2.94525367	0.00080557	3.93846129
Q20	0	5	1.26784591	4.61315956	4.82008541
Q21	0	5	1.96339766	4.74407654	3.59573276
Q23	0	5	0.95612909	4.91437612	1.16709092
Q24	0	5	2.19489458	4.99947904	1.92027109
Q29	0	5	2.20730153	4.87563351	2.73939185
Fitness value					
TVD (p.u.)	NA	NA	0.12282854	0.12260032	0.12241340
Generator reactive power (MVAr)					
QG1	-29.8	59.6	-25.7606	-28.5031	-29.6512
QG2	-24	48	-1.05136	1.95537	0.502380
QG5	-30	60	29.7033	28.3853	30.38940
QG8	-26.5	53	42.0264	43.1602	41.40386
QG11	-7.5	15	-5.16565	-3.27645	-5.020564
QG13	-7.8	15.5	6.80599	5.59714	9.579957

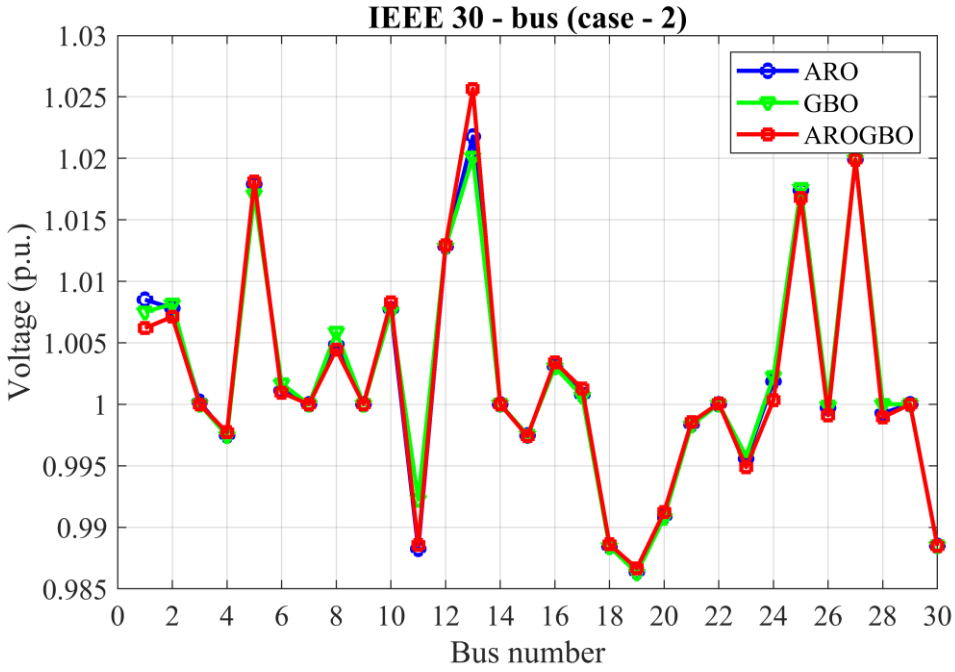

Figure 13. Voltage profile based on all algorithms for case 2.

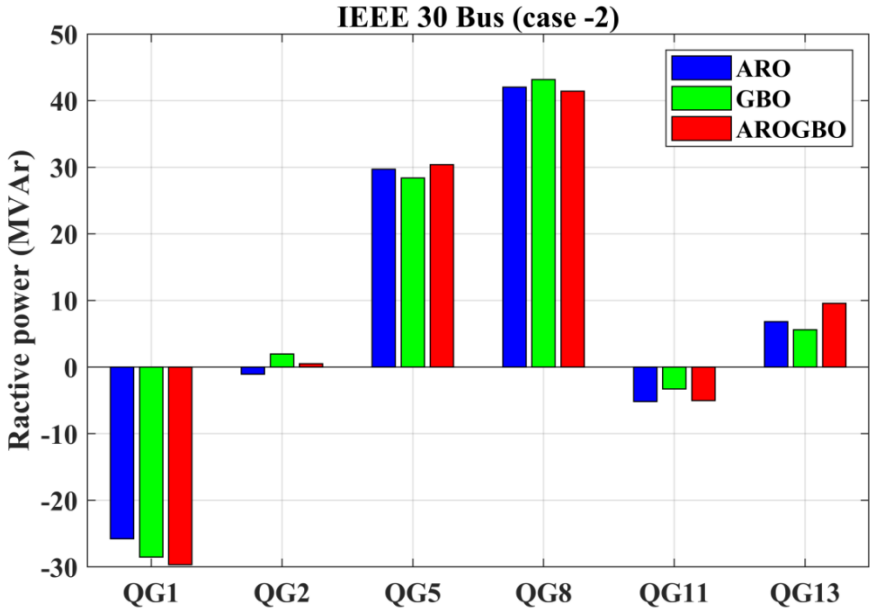

Figure 14. Reactive power generation at the generator buses based on all algorithms for case 2.

Table 10. Comparison of the attainments of AROGBO algorithm with other algorithms for case 2.

Case -2		
Algorithm	**Min**	**Mean**
SF-DE [24]	0.1231	0.1243
PDO [54]	0.14101	23.85192
SP-DE[24]	0.1224	0.1238
RSO [54]	0.29362	194.90665
EC-DE[24]	0.1217	0.1235
ROA [54]	0.12671	5.888400
SR-DE[24]	0.123	0.1241
SPO [54]	0.12477	6.740770

ECHT-DE[24]	0.1229	0.1239
PGSWT-PSO [43]	0.1539	0.2189
HAS[56]	0.1349	-
PSO-TVAC [43]	0.2064	0.2376
SGA[56]	0.1501	-
GA [20]	0.3732	-
GSA-CSS[57]	0.1239	-
SPSO-TVAC [43]	0.1354	0.1558
TS[58]	0.1540	-
FA[59]	1.9542	-
PSO [20]	0.2816	-
SWT-PSO [43]	0.1614	0.1814
PSOGWO [20]	0.278	-
PSO-CF [43]	0.1287	0.1557
ARO	0.1228300	0.1253405
GBO	0.1226000	0.1240900
AROGBO	0.1224100	0.1244380

Case - 3

In this section, the outcomes of three optimization techniques, ARO, GBO, and hybrid AROGBO, are presented for solving the reactive power dispatch problem in the IEEE 57-bus test system. The objective function used in this study is the minimization of the total power losses in the system. Figure 15 shows the single-line diagram of the proposed IEEE-57 bus test system, while Figure 16 illustrates the values of the objective function obtained from the 20 individual runs of all algorithms. The statistical analysis of the results obtained from the 20 runs for each algorithm is presented in Table 11, demonstrating the robustness and reliability of the developed hybrid AROGBO methodology. The effectiveness of the proposed AROGBO algorithm is further validated by the boxplot representation of the results, as shown in Figure 17. The convergence trends of the three algorithms are depicted in Figure 18, demonstrating that the proposed AROGBO method achieved the minimum value of the objective function in fewer iterations compared to the other methods. Table 12 presents the results of the optimization process for the best run within the 20 runs of the three algorithms. It is evident from Table 12 that the AROGBO approach attained the optimal value of power losses in the IEEE 57-bus system.

In Figure 19, the voltage magnitude at the 30 buses of the system obtained from all methods is displayed. It is evident that the voltage profile achieved using the AROGBO methodology is superior to the other techniques. The values of the reactive power generation from the six generators in the IEEE 30-bus system, as reported in Table 12, are shown graphically in Figure 20. Furthermore, to further validate the results obtained using the AROGBO methodology, they were compared with recent optimization methods employed for

addressing the RPD issue in the IEEE 57-bus system. The results of this comparison are presented in Table 10, from which it can be inferred that the AROGBO algorithm generated the lowest Ploss value among all the algorithms included in the study.

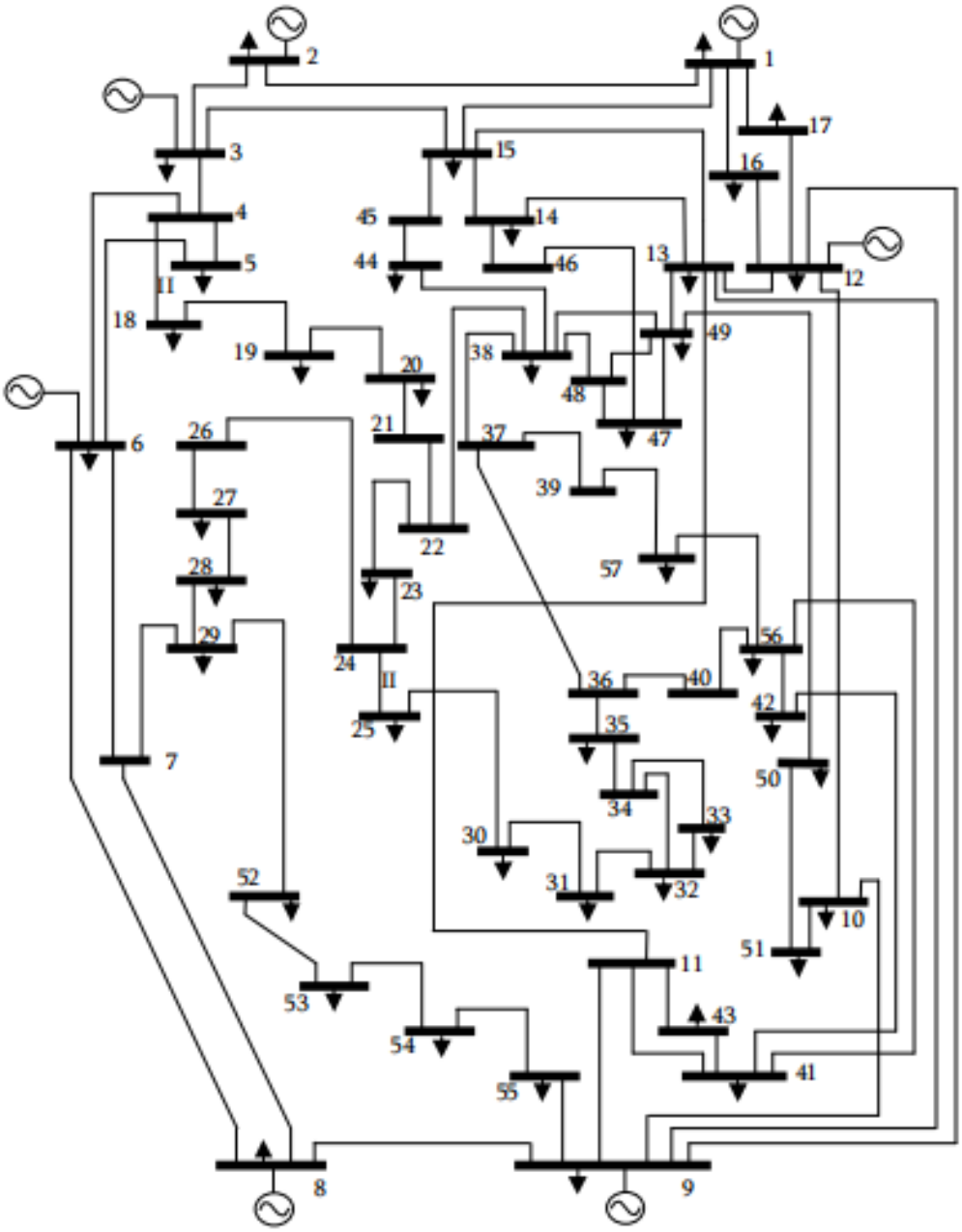

Figure 15. Single line representation of the IEEE 57-bus test system.

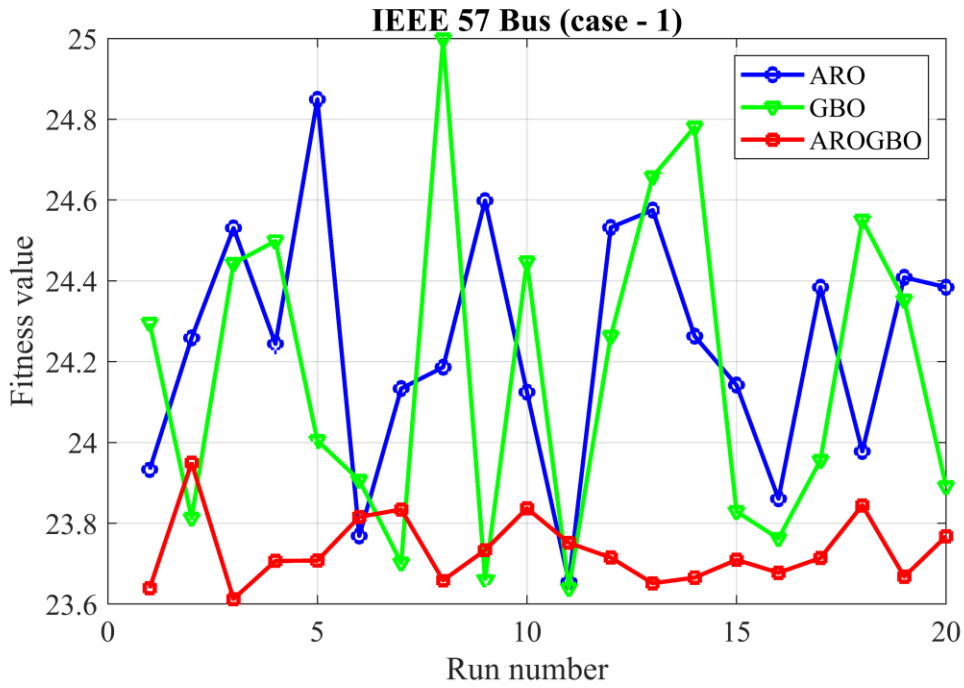

Figure 16. Best value of the objective function for all algorithms (case 3).

Table 11. Statistical results based on the 20 runs for all algorithms (case 3).

IEEE 57 Bus (Case-3)			
	ARO	**GBO**	**AROGBO**
Best	23.6549000	23.6390000	23.6126000
Worst	24.8491000	24.9992000	23.9492000
Mean	24.2405050	24.1726150	23.7329000
Median	24.2514000	24.1338500	23.7116500
SD	0.3044414	0.4072185	0.0853864
RE	0.4951236	0.0000000	0.1018948
MAE	0.5856050	0.0000000	0.1203000
RMSE	0.6564934	0.6650417	0.1462819

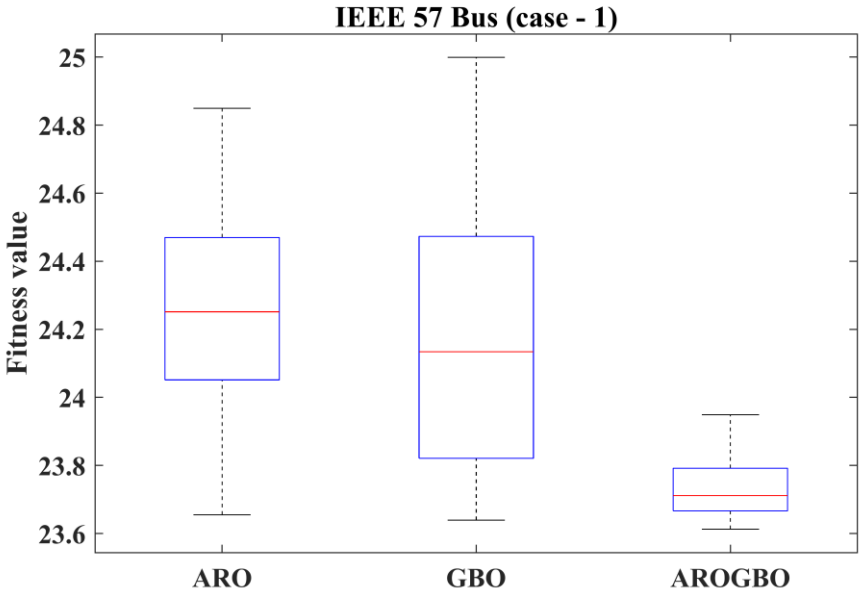

Figure 17. Boxplot representation for the results of the 20 run from all algorithms for case 3.

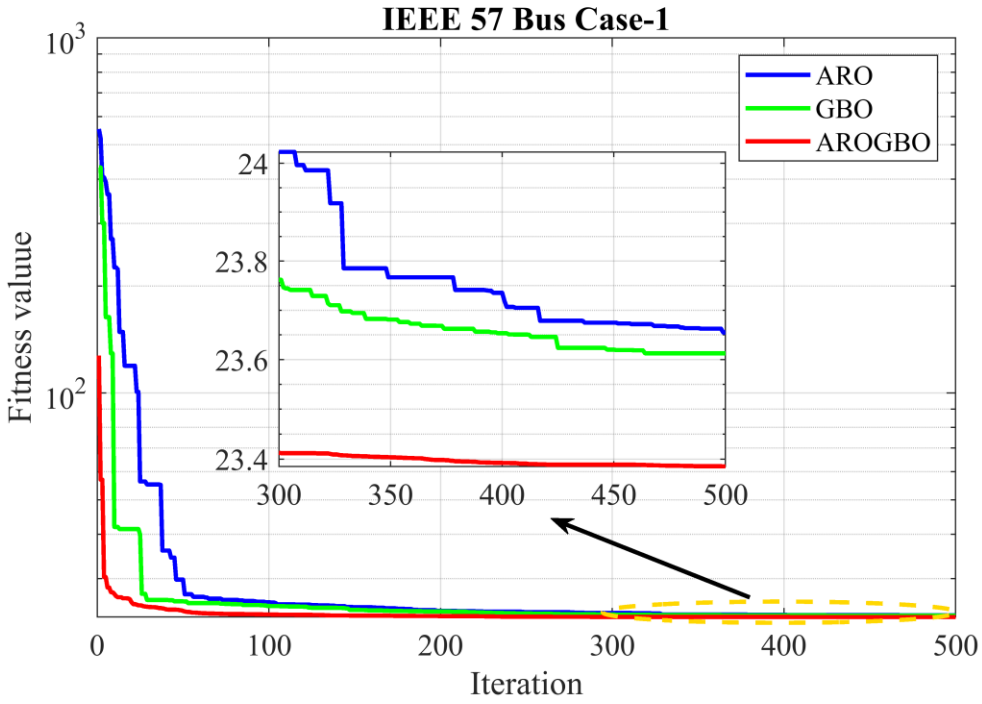

Figure 18. Convergence trends for all techniques for case - 3.

Table 12. Results of the optimization process for case -3.

	Case-3 (min P_{losses})				
Parameter	Min.	Max.	ARO	GBO	AROGBO
Generator voltage (p.u.)					
V1	0.95	1.10	1.083217285	1.09030102	1.085963448
V2	0.95	1.10	1.069314874	1.07712293	1.07312004
V3	0.95	1.10	1.049940048	1.05783667	1.055475317
V6	0.95	1.10	1.045941824	1.04068505	1.039919465
V8	0.95	1.10	1.070671497	1.05823343	1.054865735
V9	0.95	1.10	1.039683414	1.03201499	1.031919558

V12	0.95	1.10	1.049229993	1.04067699	1.047368497
Transformer Tap ratio (p.u.)					
T19	0	20	11.27860151	15.7517097	11.09040484
T20	0	20	11.11236347	9.31579773	13.24494745
T31	0	20	11.86533292	14.5636161	11.71574646
T35	0	20	11.6973468	3.66983053	8.224352442
T36	0	20	8.769054584	12.5523089	14.69603403
T37	0	20	9.932767943	10.4129675	10.24006369
T41	0	20	9.176293972	8.43632282	7.949689486
T46	0	20	6.831841197	3.18706932	6.736623212
T54	0	20	4.777515965	2.78499750	2.603273016
T58	0	20	7.986035535	7.83801020	8.309964543
T59	0	20	6.498760502	9.10552379	6.983301956
T65	0	20	8.653286019	8.51305067	7.191308636
T66	0	20	4.47093636	4.09916654	3.537023815
T71	0	20	7.224761365	11.6820520	7.415049555
T73	0	20	8.557723065	11.3895202	6.249994992
T76	0	20	7.245265292	8.68096476	8.595063279
T80	0	20	8.984357751	7.28813058	8.74584999
Capacitor Bank (MVAr)					
Q18	0	20	15.1718178	8.26784375	16.86837323
Q25	0	20	12.76350579	11.2739782	14.61355041
Q53	0	20	15.77466951	20.3806696	15.05211312
Fitness value					
P_{losses} (MW)	NA	NA	23.65493946	23.7331754	23.61263989
Generator reactive power (MVAr)					
QG1	-140	200	63.47223	77.29651	63.104611
QG2	-17	50	47.72461	49.99878	49.46717
QG3	-10	60	15.91929	43.24213	32.17996
QG6	-8	25	-6.339425	-6.750817	-4.393956
QG8	-140	200	72.83576	52.45729	44.02671
QG9	-3	9	2.975921	9.000768	8.601342
QG12	-150	155	69.23581	47.88880	70.25194

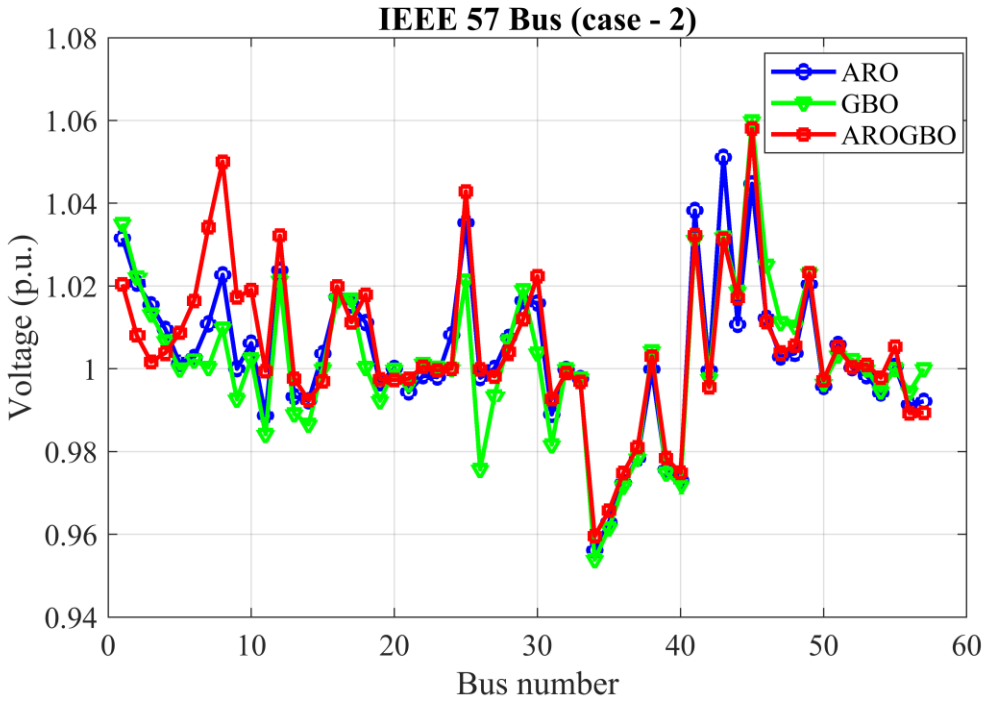

Figure 19. Voltage profile based on all algorithms for case 2.

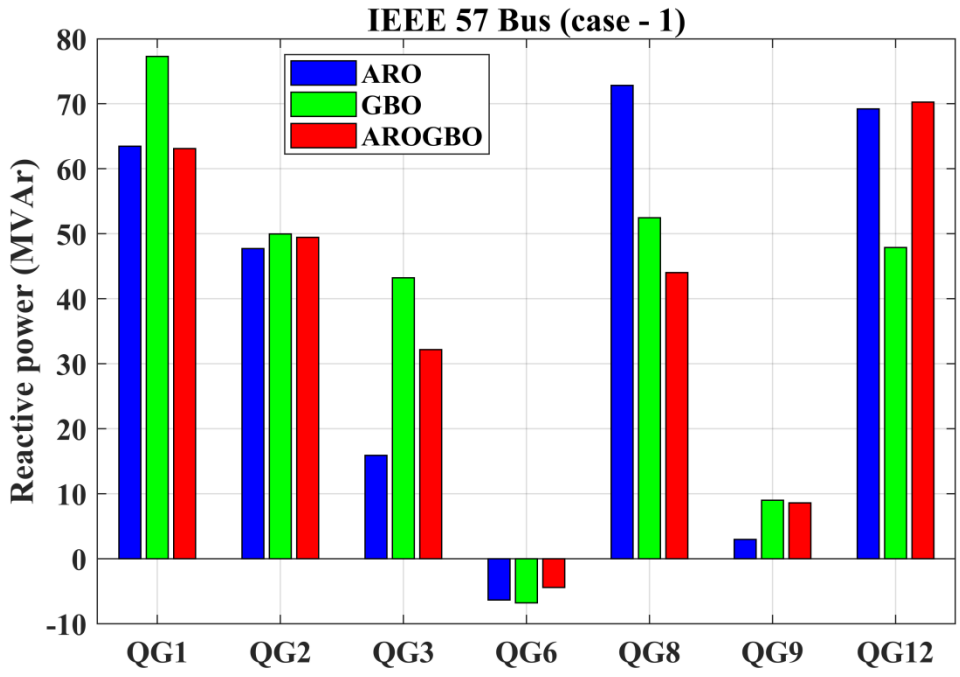

Figure 20. Reactive power generation at the generator buses based on all algorithms for case 2.

Table 12. Comparison of the attainments of AROGBO algorithm with other algorithms for case 2.

Case -3		
Algorithm	**Min**	**Mean**
SF-DE [24]	23.363	23.7164
PDO [54]	50.57143	-
SP-DE[24]	23.35	23.6954
RSO [54]	32.60550	-
EC-DE[24]	23.34	23.792

AVOA [54]	27.51680	-
SR-DE[24]	23.355	23.4392
ROA [54]	47.24557	-
ECHT-DE[24]	23.396	23.4963
SPO [54]	39.26724	-
PSO [46]	24.3826	-
ABC [60]	24.102	-
SGA [47]	23.836	24.5448
MCBOA [46]	23.9643	-
CGA [60]	25.744	-
PSO-ICA [50]	24.1386	-
HAS [60]	24.501	-
BA [11]	24.9254	-
CLPSO [60]	24.515	-
BSO [48]	24.3744	-
MOGWA [49]	23.71544	-
ALC-PSO [51]	23.39	23.41
GSA [46]	24.4922	-
ICA [50]	24.1607	-
CSA [46]	24.2619	-
MOALO [52]	26.539	-
MFOM [11]	24.25293	-
WCA [45]	24.82	-
FBA [11]	24.8419	-
ARO	23.6549000	24.2405050
GBO	23.6390000	23.7342200
AROGBO	23.6126000	24.1712950

Case - 4

This subsection presents the results of various methodologies used to optimize the RPD issue in the IEEE 57-bus test system. The objective function used is the minimization of total voltage deviations (TVD) at all buses. Figure 21 illustrates the 20 values of the objective function obtained from 20 individual runs of the three algorithms. Table 13 reports the statistical results of the 20 implementations for all techniques. The proposed hybrid AROGBO algorithm is shown to be accurate and robust based on the results of both parametric and non-parametric statistical metrics, as demonstrated in Figure 22. The convergence trends of the three techniques for the fourth case study are presented in Figure 23, and Table 14 lists the optimized variables from the proposed ARO, GBO, and hybrid AROGBO techniques. It is evident from Table 14 that the AROGBO method achieved the lowest value of total voltage deviations in the system, thereby validating the effectiveness of the proposed algorithm.

Figure 24 displays the voltage magnitude at the 57 buses of the power system. Among the considered algorithms, the voltage profile obtained by the developed AROGBO methodology is the best. The reactive power generation values of the six generators included in the IEEE 57-bus system are presented in graphical form in Figure 25 and reported in Table 14. To further validate the proposed hybrid AROGBO algorithm, its results are compared with recent optimization techniques applied to solve the RPD issue in the IEEE 57-bus system, as reported in Table 15. The proposed AROGBO algorithm achieves the minimum value of the objective function.

Considering the results of the four case studies, it is evident that the proposed hybrid AROGBO algorithm outperforms the conventional ARO and GBO algorithms, as well as other recent optimization techniques used to address the optimization problem of reactive power dispatch in power systems.

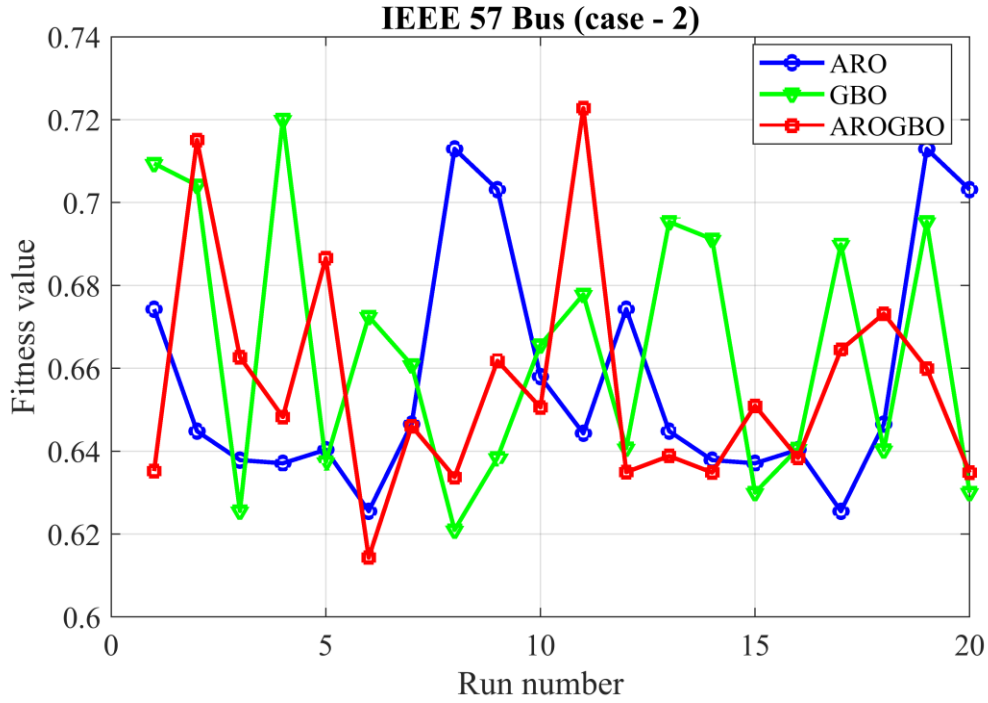

Figure 21. Best value of the objective function for all algorithms (case 4).

Table 13. Statistical results based on the 20 runs for all algorithms (case 4).

IEEE 57 Bus (Case-4)			
	ARO	**GBO**	**AROGBO**
Best	0.6255100	0.6209800	0.6143200
Worst	0.7129500	0.7200900	0.7227600
Mean	0.6573635	0.6643115	0.6553705
Median	0.6448200	0.6632300	0.6494150
SD	0.0288873	0.0317259	0.0272986
RE	1.0184809	1.2480756	0.0000000
MAE	0.0318535	0.0387515	0.0000000

RMSE	0.0425135	0.0495771	0.0489193

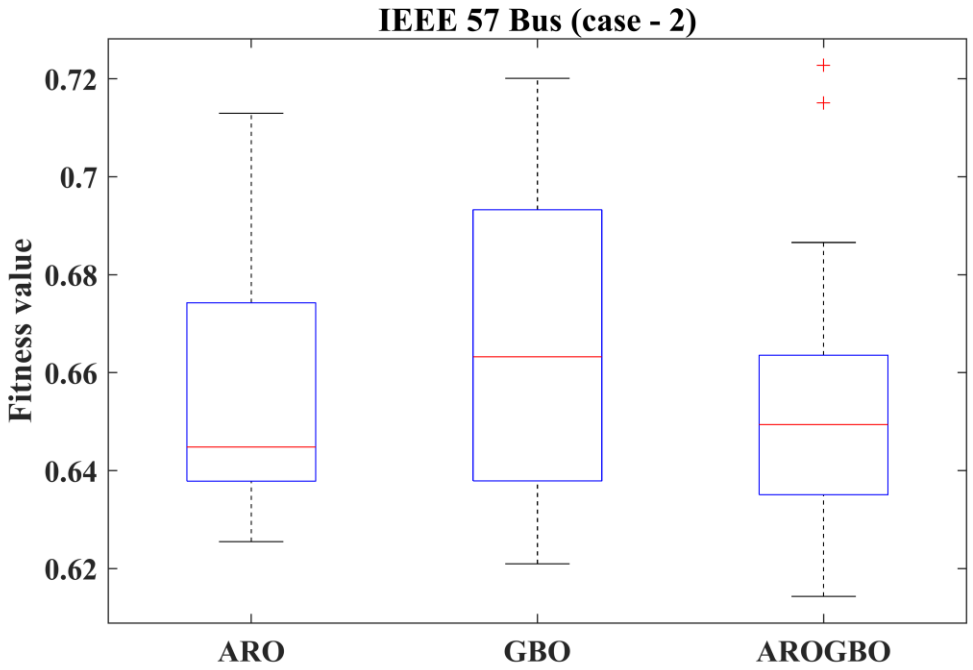

Figure 22. Boxplot representation for the results of the 20 run from all techniques for case 4.

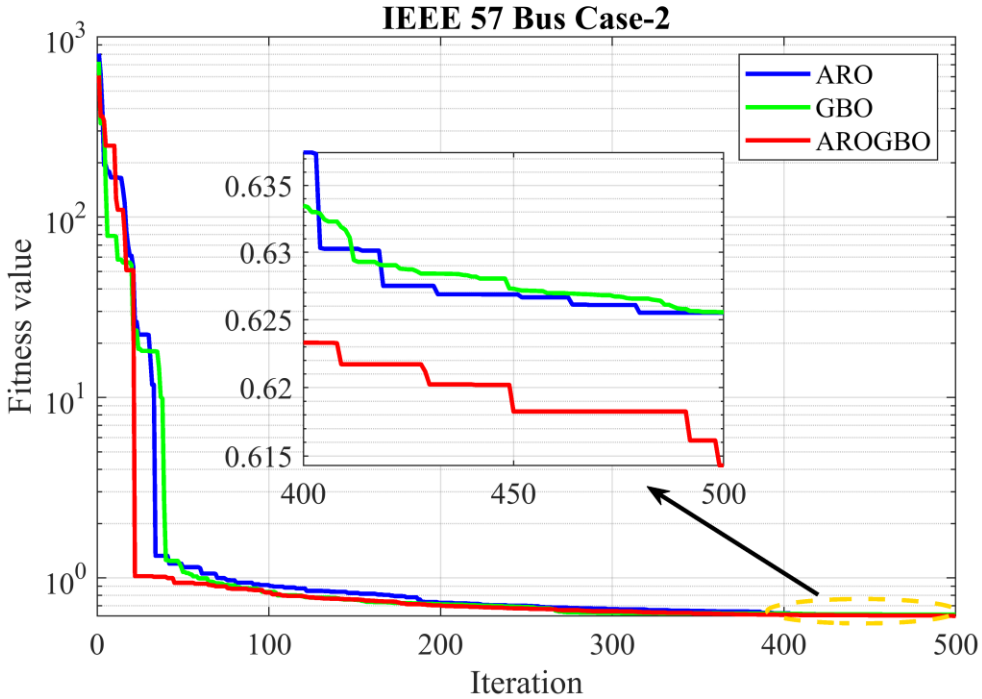

Figure 23. Convergence trends of all techniques for case 4.

Table 14. Results of the optimization process for case 4.

	Case -4 (min VD)				
Parameter	Min.	Max.	ARO	GBO	AROGBO
Generator voltage (p.u.)					
V1	0.950	1.10	1.020408853	1.035109604	1.031603234

V2	0.950	1.10	1.008048429	1.022182552	1.020699782
V3	0.950	1.10	1.001658711	1.013256277	1.015450669
V6	0.950	1.10	1.01641168	1.002082969	1.002738162
V8	0.950	1.10	1.050062631	1.009829564	1.022702052
V9	0.950	1.10	1.01730096	0.992637971	1.000013746
V12	0.950	1.10	1.03214478	1.021397417	1.023845424
Transformer Tap ratio (p.u.)					
T19	0	20	11.12101378	16.97912796	5.273183873
T20	0	20	6.497353041	4.772783833	13.60824675
T31	0	20	8.74440096	7.410670709	7.688756983
T35	0	20	17.02597478	19.99566078	12.42190202
T36	0	20	7.784371333	1.333227563	18.79265183
T37	0	20	9.699105607	12.4769249	10.74928061
T41	0	20	12.66378808	8.069397857	9.726606074
T46	0	20	3.906197069	2.04003401	3.115516749
T54	0	20	0.172435622	8.29E-07	0.197814539
T58	0	20	3.052294774	3.103815893	5.285401368
T59	0	20	8.244717424	5.73484055	7.938936459
T65	0	20	11.09014096	9.660597817	9.711915843
T66	0	20	0.24796427	5.21E-06	0.278714611
T71	0	20	6.739627649	5.163067832	3.450949845
T73	0	20	10.41853179	9.984291837	11.60216451
T76	0	20	3.329637839	0.005214171	2.440102853
T80	0	20	11.31082456	9.411231811	10.06096914
Capacitor Bank (MVAr)					
Q18	0	20	10.36980891	6.183358567	9.529746382
Q25	0	20	18.64950935	11.49767637	20.95659224
Q53	0	20	27.55060788	25.75227344	26.1086418
Fitness value					
TVD (p.u.)	NA	NA	0.625509635	0.625557386	0.614324897
Generator reactive power (MVAr)					
QG1	-140	200	6.156874	38.62658	19.10408
QG2	-17	50	41.93380	41.89747	45.12042
QG3	-10	60	17.89956	54.79744	54.87256
QG6	-8	25	-3.237063	11.52794	-7.972896
QG8	-140	200	78.69495	21.04994	42.75984
QG9	-3	9	6.575325	8.752423	6.651032
QG12	-150	155	134.2319	120.0509	118.8791

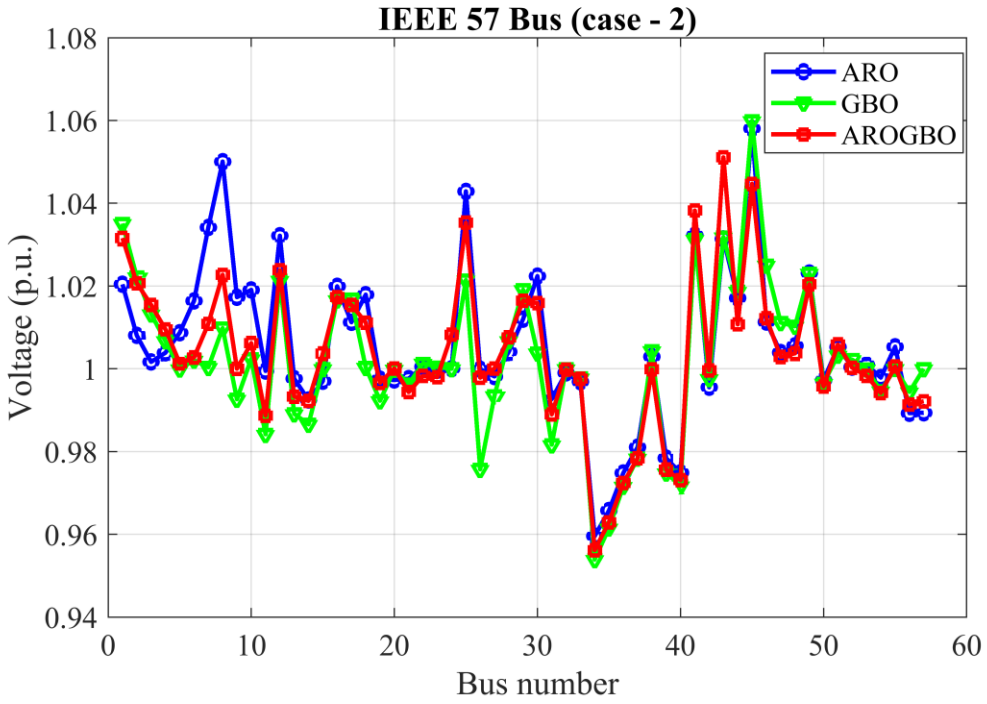

Figure 24. Voltage profile based on all algorithms for case 4.

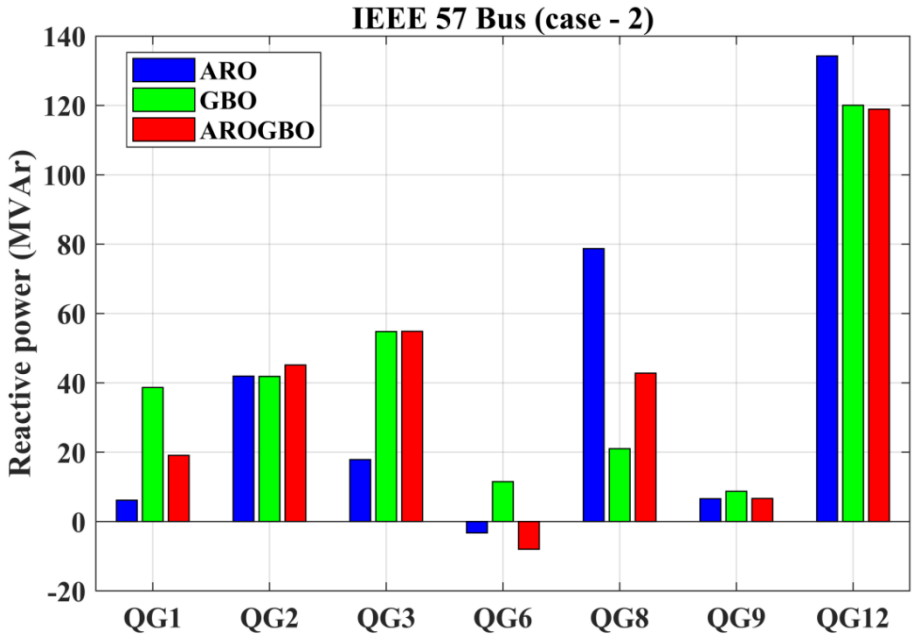

Figure 25. Reactive power generation at the generator buses based on all algorithms for case 4.

Table 15. Comparison of the attainments of AROGBO method with recent methods for case 4.

Case -4		
Algorithm	**Min**	**Mean**
SF-DE [24]	0.586	0.6077
ASNS[61]	0.6405	0.6653
SP-DE[24]	0.589	0.6085
SNS[61]	0.6520	0.7018
EC-DE[24]	0.59	0.6173
OGSA[62]	0.6982	-

SR-DE[24]	0.59	0.6069
GB-WCA[63]	0.6501	-
ECHT-DE[24]	0.588	0.6073
WCA[63]	0.6631	-
ALC-PSO [51]	0.6634	0.6686
NGWCA [45]	0.6501	-
BA [33]	0.6434	0.6499
OGSA [53]	0.6982	-
CBA-III [33]	0.6413	0.644
WCA [45]	0.6631	-
ALO [44]	0.6666	0.7534
CBA-IV [33]	0.6399	0.6424
GBWCA [45]	0.6501	-
ARO	0.6255100	0.6573635
GBO	0.6255600	0.6559325
AROGBO	0.6143200	0.6637495

Case – 5

In this section, we delve into the comparative analysis ARO), GBO, and the developed hybrid AROGBO. The focus of this evaluation is on their application to solve the reactive power dispatch problem within the complex framework of the IEEE 118-bus test system. The primary goal of this study is the minimization of total power losses in the system.

The convergence trends of the three algorithms are visually represented in Figure 26, providing a clear insight into their performance dynamics. Notably, the AROGBO method stands out by achieving the minimum value of the objective function in significantly fewer iterations compared to its counterparts. The convergence graph showcases that the AROGBO algorithm reached an impressive minimum value of power losses at 212.5479 MW, outperforming both ARO and GBO, which achieved 221.6818 MW and 213.5311 MW, respectively. Table 16 further details the outcomes of the optimization process for each algorithm, affirming that the AROGBO approach excelled in attaining the optimal value of power losses within the IEEE 118-bus system. This numerical representation solidifies the superiority of the hybrid AROGBO method in addressing the reactive power dispatch problem. To gain a comprehensive understanding of the system's behavior, Figure 26 also presents the voltage magnitude at the 118 buses obtained from all three optimization techniques. The visualization unequivocally demonstrates that the voltage profile derived through the AROGBO methodology surpasses those produced by the other algorithms. This enhancement in voltage magnitude not only signifies the efficacy of the AROGBO approach in minimizing power losses but also highlights its capacity to maintain a superior voltage profile throughout the IEEE 118-bus system.

In conclusion, the extensive application of the hybrid AROGBO algorithm on the IEEE 118-bus test system has demonstrated its prowess in efficiently solving the reactive power dispatch problem. The superior convergence speed and the attainment of the optimal power loss value underscore the effectiveness of the AROGBO approach. Additionally, the enhanced voltage profile further solidifies the conclusion that the developed hybrid algorithm outperforms both ARO and GBO in addressing the complexities of the power system. The results substantiate the practical applicability and efficiency of the AROGBO methodology, positioning it as a promising solution for real-world power system optimization challenges.

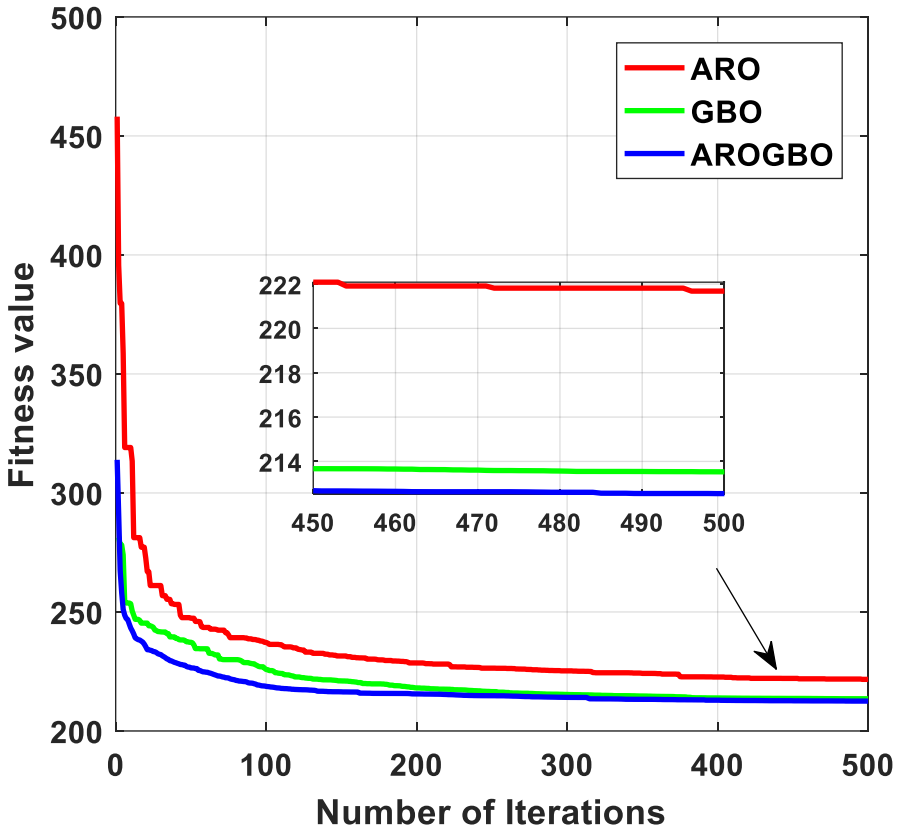

Figure 26. Convergence trends of all techniques for case 4.

Table 16 Numerical results of studied algorithms for IEEE118-bus system

Control Variables	Min.	Max.	ARO	GBO	AROGBO
Generator voltage					
V1	0.95	1.1	1.008215	1.039971	1.032171
V4	0.95	1.1	1.038864	1.07091	1.064512
V6	0.95	1.1	1.035179	1.064256	1.054022
V8	0.95	1.1	1.056897	1.067044	1.080974
V10	0.95	1.1	1.058032	1.086409	1.099989

V12	0.95	1.1	1.036798	1.059385	1.051917
V15	0.95	1.1	1.033458	1.054199	1.047092
V18	0.95	1.1	1.034823	1.057835	1.050369
V19	0.95	1.1	1.029289	1.053061	1.045612
V24	0.95	1.1	1.030076	1.057161	1.059882
V25	0.95	1.1	1.060392	1.091025	1.085859
V26	0.95	1.1	1.028002	1.067736	1.099996
V27	0.95	1.1	1.019517	1.063793	1.052519
V31	0.95	1.1	1.025309	1.052915	1.04426
V32	0.95	1.1	1.019264	1.058237	1.049117
V34	0.95	1.1	1.043369	1.056142	1.050266
V36	0.95	1.1	1.039937	1.051301	1.048518
V40	0.95	1.1	1.039858	1.055795	1.039298
V42	0.95	1.1	1.046012	1.059359	1.047432
V46	0.95	1.1	1.036487	1.062103	1.06267
V49	0.95	1.1	1.050624	1.070417	1.07588
V54	0.95	1.1	1.024887	1.05276	1.057902
V55	0.95	1.1	1.023181	1.049932	1.056611
V56	0.95	1.1	1.02407	1.050564	1.056678
V59	0.95	1.1	1.05572	1.062585	1.075996
V61	0.95	1.1	1.064203	1.048084	1.075316
V62	0.95	1.1	1.056799	1.047432	1.072568
V65	0.95	1.1	1.056001	1.099898	1.080484
V66	0.95	1.1	1.05145	1.071531	1.081666
V69	0.95	1.1	1.055617	1.086776	1.080616
V70	0.95	1.1	1.027578	1.063259	1.04386
V72	0.95	1.1	1.022977	1.062605	1.046244
V73	0.95	1.1	1.03109	1.065041	1.043774
V74	0.95	1.1	1.015276	1.049101	1.024112
V76	0.95	1.1	1.006725	1.02587	1.009978
V77	0.95	1.1	1.036933	1.059054	1.04959
V80	0.95	1.1	1.04703	1.066979	1.060073
V85	0.95	1.1	1.037827	1.065986	1.065966
V87	0.95	1.1	1.027797	1.045617	1.036442
V89	0.95	1.1	1.054586	1.096532	1.08787
V90	0.95	1.1	1.03348	1.069123	1.055939
V91	0.95	1.1	1.028166	1.070716	1.054342
V92	0.95	1.1	1.037748	1.076108	1.066527
V99	0.95	1.1	1.051804	1.066451	1.056518
V100	0.95	1.1	1.046832	1.070407	1.064698
V103	0.95	1.1	1.050758	1.067683	1.061209
V104	0.95	1.1	1.041704	1.056635	1.052798
V105	0.95	1.1	1.042587	1.054863	1.051929
V107	0.95	1.1	1.021398	1.041059	1.073828
V110	0.95	1.1	1.042425	1.059747	1.043922
V111	0.95	1.1	1.04095	1.070286	1.062436
V112	0.95	1.1	1.049557	1.050242	1.026316
V113	0.95	1.1	1.050535	1.068765	1.062237
V116	0.95	1.1	1.045581	1.0913	1.069972

Transformer tap ratio

T8-5	0.9	1.1	1.044995	0.979964	1.008579
T26-25	0.9	1.1	0.98778	0.978762	1.0186
T30-17	0.9	1.1	0.975744	0.995008	1.008276
T38-37	0.9	1.1	0.984203	0.998675	0.998585
T63-59	0.9	1.1	1.015341	1.017247	0.979523
T64-61	0.9	1.1	1.006232	1.042433	0.997102
T65–66	0.9	1.1	1.007723	1.027589	1.000975
T68–69	0.9	1.1	1.003431	0.998648	0.981182
T81-80	0.9	1.1	1.001527	1.022107	0.991149
Capacitor bank					
QC5	-30	30	-1.46175	-25.0384	-2.83368
QC34	-30	30	-9.71152	20.68622	-12.6854
QC37	-30	30	3.703024	-30	-1.27002
QC44	-30	30	-12.5152	1.15328	0.601268
QC45	-30	30	7.460292	23.12554	23.09616
QC46	-30	30	-1.04036	-29.9714	-4.839
QC48	-30	30	0.098809	16.33003	10.09446
QC74	-30	30	27.46936	28.52816	10.50428
QC79	-30	30	20.25326	29.71859	29.94621
QC82	-30	30	-4.19139	25.81295	21.37861
QC83	-30	30	24.33027	25.55878	16.55738
QC105	-30	30	29.29418	29.98984	-3.18327
QC107	-30	30	-7.2023	-29.9983	-1.47672
QC110	-30	30	-5.90379	24.11172	-2.51512
Objective function					
P_{Loss} (MW)			221.6818	213.5311	212.5479

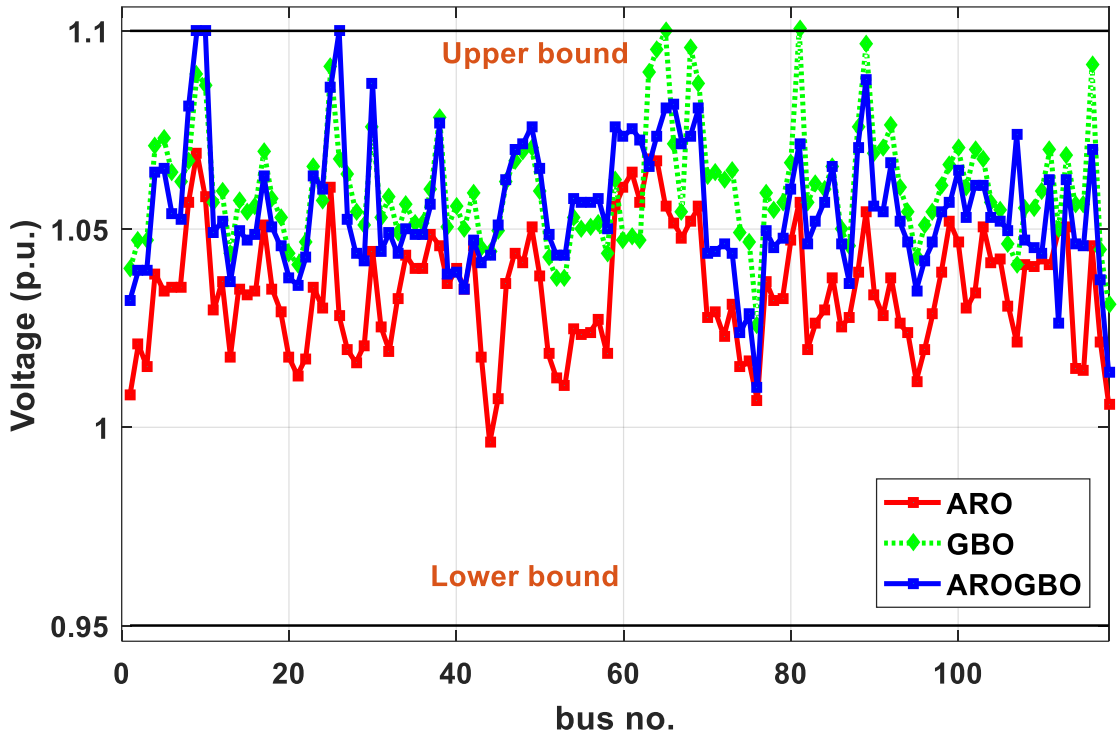

Figure 27 Voltage profiles of Load buses for the 118-bus system

5. Conclusion

In this study, a new hybrid optimization algorithm called AROGBO, based on the combination of ARO and GBO algorithms, has been developed and applied to solve the ORPD problem in electrical networks. The effectiveness of the proposed algorithm was tested utilizing standard test systems (IEEE-30 bus, IEEE-57 bus, and IEEE-118 bus) and two objective functions were considered: minimizing the total power losses in the system and minimizing the total voltage deviations at the buses. Statistical analysis showed that the AROGBO technique is accurate and stable in all cases included in this work. In all case studies, the AROGBO algorithm outperformed the standard ARO and GBO algorithms as well as recent optimization techniques used for ORPD. Specifically, the AROGBO algorithm obtained the best values of the objective function. For example, in case 1, the minimum power loss was 4.945088 MW for AROGBO, while it was 4.94516 MW for ARO and 4.94524 MW for GBO. Similarly, in case 2, the minimum total voltage deviation was 0.122413 p.u. for AROGBO, while it was 0.122829 p.u. for ARO and 0.1226 p.u. for GBO. These results demonstrate the superiority of AROGBO in solving ORPD problems. In future works, the AROGBO algorithm can be adapted to handle such multi-objective scenarios, aiming to strike a balance between competing goals, such as cost reduction, improved voltage stability, and reduced power losses.

Conflict of interest The authors declare that there is no conflict of interest regarding the publication of this manuscript.

References

[1] M. G. Gafar, R. A. El-Sehiemy, and H. M. Hasanien, "A novel hybrid fuzzy-JAYA optimization algorithm for efficient ORPD solution," *IEEE Access,* vol. 7, pp. 182078-182088, 2019.

[2] R. H. Salimin *et al.*, "Multi cases optimal reactive power dispatch using evolutionary programming," *Indonesian Journal of Electrical Engineering and Computer Science (IJEECS),* vol. 17, no. 2, pp. 662-670, 2020.

[3] S. K. ElSayed and E. E. Elattar, "Slime mold algorithm for optimal reactive power dispatch combining with renewable energy sources," *Sustainability,* vol. 13, no. 11, p. 5831, 2021.

[4] Y. Muhammad, R. Khan, F. Ullah, A. u. Rehman, M. S. Aslam, and M. A. Z. Raja, "Design of fractional swarming strategy for solution of optimal reactive power dispatch," *Neural Computing and Applications,* vol. 32, pp. 10501-10518, 2020.

[5] E. Yalcin, M. C. TAPLAMACIOĞLU, and Ç. Ertuğrul, "The adaptive chaotic symbiotic organisms search algorithm proposal for optimal reactive power dispatch problem in power systems," *Electrica,* vol. 19, no. 1, pp. 37-47, 2019.

[6] P. Ramkee, S. Chaitanya, B. Venkateswara Rao, and R. Ashok Bakkiyaraj, "Optimal Reactive Power Dispatch Under Load Uncertainty Incorporating Solar Power Using Firefly Algorithm," in *Advances in Energy Technology: Select Proceedings of EMSME 2020*, 2022, pp. 423-434: Springer.

[7] A. M. Abd-El Wahab, S. Kamel, M. H. Hassan, M. I. Mosaad, and T. A. AbdulFattah, "Optimal Reactive Power Dispatch Using a Chaotic Turbulent Flow of Water-Based Optimization Algorithm," *Mathematics,* vol. 10, no. 3, p. 346, 2022.

[8] R. Chi, Z. Li, X. Chi, Z. Qu, and H.-b. Tu, "Reactive power optimization of power system based on improved differential evolution algorithm," *Mathematical Problems in Engineering,* vol. 2021, pp. 1-19, 2021.

[9] M. Sabir, A. Ahmad, A. Ahmed, S. Siddique, and U. A. Hashmi, "A modified inertia weight control of particle swarm optimization for optimal reactive power dispatch problem," in *2021 International Conference on Emerging Power Technologies (ICEPT)*, 2021, pp. 1-6: IEEE.

[10] L. C. Kien, C. T. Hien, and T. T. Nguyen, "Optimal reactive power generation for transmission power systems considering discrete values of capacitors and tap changers," *Applied Sciences,* vol. 11, no. 12, p. 5378, 2021.

[11] R. N. S. Mei, M. H. Sulaiman, Z. Mustaffa, and H. Daniyal, "Optimal reactive power dispatch solution by loss minimization using moth-flame optimization technique," *Applied Soft Computing,* vol. 59, pp. 210-222, 2017.

[12] M. Ghasemi, M. M. Ghanbarian, S. Ghavidel, S. Rahmani, and E. M. Moghaddam, "Modified teaching learning algorithm and double differential evolution algorithm for optimal reactive power dispatch problem: a comparative study," *Information Sciences,* vol. 278, pp. 231-249, 2014.

[13] M. H. Hassan, S. Kamel, M. A. El-Dabah, T. Khurshaid, and J. L. Domínguez-García, "Optimal reactive power dispatch with time-varying demand and renewable energy uncertainty using Rao-3 algorithm," *IEEE Access,* vol. 9, pp. 23264-23283, 2021.

[14] R. Roy, T. Das, and K. K. Mandal, "Optimal reactive power dispatch using a novel optimization algorithm," *Journal of Electrical Systems and Information Technology,* vol. 8, no. 1, pp. 1-24, 2021.

[15] T. Das, R. Roy, and K. K. Mandal, "Solving optimal reactive power dispatch problem with the consideration of load uncertainty using modified JAYA algorithm," in *2021 International Conference on Advances in Electrical, Computing, Communication and Sustainable Technologies (ICAECT)*, 2021, pp. 1-6: IEEE.

[16] D. Londono, V. Acevedo, and J. López-Lezama, "Mean-Variance Mapping Optimization Algorithm Applied to the Optimal Reactive Power Dispatch [J]," *Inge CUC,* vol. 17, no. 1, pp. 1-1, 2021.

[17] S. K. Elsayed, S. Kamel, A. Selim, and M. Ahmed, "An improved heap-based optimizer for optimal reactive power dispatch," *IEEE Access,* vol. 9, pp. 58319-58336, 2021.

[18] A. Mukherjee and V. Mukherjee, "Solution of optimal reactive power dispatch by chaotic krill herd algorithm," *IET Generation, Transmission & Distribution,* vol. 9, no. 15, pp. 2351-2362, 2015.

[19] N. V. Korovkin, K. Ahmed Mamdouh, and H. Osman Mohamed, "Optimal reactive power dispatch in power system comprising renewable energy sources by means of a multi-objective particle swarm algorithm," *Global Energy,* vol. 115, no. 1, pp. 5-20, 2021.

[20] M. A. Shaheen, H. M. Hasanien, and A. Alkuhayli, "A novel hybrid GWO-PSO optimization technique for optimal reactive power dispatch problem solution," *Ain Shams Engineering Journal,* vol. 12, no. 1, pp. 621-630, 2021.

[21] M. Ebeed, A. Alhejji, S. Kamel, and F. Jurado, "Solving the optimal reactive power dispatch using marine predators algorithm considering the uncertainties in load and wind-solar generation systems," *Energies*, vol. 13, no. 17, p. 4316, 2020.
[22] Y. Zhou, J. Zhang, X. Yang, and Y. Ling, "Optimal reactive power dispatch using water wave optimization algorithm," *Operational Research*, vol. 20, pp. 2537-2553, 2020.
[23] H. Yapici, "Solution of optimal reactive power dispatch problem using pathfinder algorithm," *Engineering Optimization*, vol. 53, no. 11, pp. 1946-1963, 2021.
[24] R. Mallipeddi, S. Jeyadevi, P. N. Suganthan, and S. Baskar, "Efficient constraint handling for optimal reactive power dispatch problems," *Swarm and Evolutionary Computation*, vol. 5, pp. 28-36, 2012.
[25] M. Kunapareddy and B. V. Rao, "Hybridization of particle swarm optimization with firefly algorithm for multi-objective optimal reactive power dispatch," in *Innovative Product Design and Intelligent Manufacturing Systems: Select Proceedings of ICIPDIMS 2019*, 2020, pp. 673-682: Springer.
[26] N. H. Khan, Y. Wang, D. Tian, M. A. Z. Raja, R. Jamal, and Y. Muhammad, "Design of fractional particle swarm optimization gravitational search algorithm for optimal reactive power dispatch problems," *IEEE Access*, vol. 8, pp. 146785-146806, 2020.
[27] R. Jamal, B. Men, N. H. Khan, M. A. Z. Raja, and Y. Muhammad, "Application of Shannon entropy implementation into a novel fractional particle swarm optimization gravitational search algorithm (FPSOGSA) for optimal reactive power dispatch problem," *IEEE Access*, vol. 9, pp. 2715-2733, 2020.
[28] N. H. Khan, Y. Wang, D. Tian, R. Jamal, M. Ebeed, and Q. Deng, "Fractional PSOGSA algorithm approach to solve optimal reactive power dispatch problems with uncertainty of renewable energy resources," *IEEE Access*, vol. 8, pp. 215399-215413, 2020.
[29] K. Rojanaworahiran and K. Chayakulkheeree, "Probabilistic optimal power flow considering load and solar power uncertainties using particle swarm optimization," *Energy*, vol. 1, no. 2,993.29, pp. 6,000, 2015.
[30] S. K. Gupta, M. K. Kar, L. Kumar, and S. Kumar, "A Simplified Sine Cosine Algorithm for the Solution of Optimal Reactive Power Dispatch," *International Transactions on Electrical Energy Systems*, vol. 2022, 2022.
[31] M. Ebeed, A. Ali, M. I. Mosaad, and S. Kamel, "An improved lightning attachment procedure optimizer for optimal reactive power dispatch with uncertainty in renewable energy resources," *IEEE Access*, vol. 8, pp. 168721-168731, 2020.
[32] T. T. Nguyen and D. N. Vo, "Improved social spider optimization algorithm for optimal reactive power dispatch problem with different objectives," *Neural Computing and Applications*, vol. 32, no. 10, pp. 5919-5950, 2020.
[33] S. Mugemanyi, Z. Qu, F. X. Rugema, Y. Dong, C. Bananeza, and L. Wang, "Optimal reactive power dispatch using chaotic bat algorithm," *IEEE Access*, vol. 8, pp. 65830-65867, 2020.
[34] L. Wang, Q. Cao, Z. Zhang, S. Mirjalili, and W. Zhao, "Artificial rabbits optimization: A new bio-inspired meta-heuristic algorithm for solving engineering optimization problems," *Engineering Applications of Artificial Intelligence*, vol. 114, p. 105082, 2022.
[35] A. O. Alsaiari, E. B. Moustafa, H. Alhumade, H. Abulkhair, and A. Elsheikh, "A coupled artificial neural network with artificial rabbits optimizer for predicting water productivity of different designs of solar stills," *Advances in Engineering Software*, vol. 175, p. 103315, 2023.
[36] Y. Wang, L. Huang, J. Zhong, and G. Hu, "LARO: Opposition-based learning boosted artificial rabbits-inspired optimization algorithm with Lévy flight," *Symmetry*, vol. 14, no. 11, p. 2282, 2022.
[37] I. Ahmadianfar, O. Bozorg-Haddad, and X. Chu, "Gradient-based optimizer: A new metaheuristic optimization algorithm," *Information Sciences*, vol. 540, pp. 131-159, 2020.
[38] A. A. Ismaeel, E. H. Houssein, D. Oliva, and M. Said, "Gradient-based optimizer for parameter extraction in photovoltaic models," *IEEE Access*, vol. 9, pp. 13403-13416, 2021.
[39] S. Deb, D. S. Abdelminaam, M. Said, and E. H. Houssein, "Recent methodology-based gradient-based optimizer for economic load dispatch problem," *IEEE Access*, vol. 9, pp. 44322-44338, 2021.
[40] H. Rezk *et al.*, "Optimal parameter estimation strategy of PEM fuel cell using gradient-based optimizer," *Energy*, vol. 239, p. 122096, 2022.
[41] A. M. Agwa, Y. I. Mesalam, M. H. Hassan, M. A. El-Dabah, A. M. El-Sherif, and S. Kamel, "Improved Gradient-Based Optimizer for Modelling Thermal and Hydropower Plants," *International Transactions on Electrical Energy Systems*, 2022.
[42] A. A. Mohamed, S. Kamel, M. H. Hassan, M. I. Mosaad, and M. Aljohani, "Optimal Power Flow Analysis Based on Hybrid Gradient-Based Optimizer with Moth–Flame Optimization Algorithm Considering Optimal Placement and Sizing of FACTS/Wind Power," *Mathematics*, vol. 10, no. 3, 2022.
[43] J. Polprasert, W. Ongsakul, and V. N. Dieu, "Optimal reactive power dispatch using improved pseudo-gradient search particle swarm optimization," *Electric Power Components and Systems*, vol. 44, no. 5, pp. 518-532, 2016.

[44] Z. Li, Y. Cao, L. V. Dai, X. Yang, and T. T. Nguyen, "Finding solutions for optimal reactive power dispatch problem by a novel improved antlion optimization algorithm," *Energies*, vol. 12, no. 15, p. 2968, 2019.

[45] A. A. Heidari, R. A. Abbaspour, and A. R. Jordehi, "Gaussian bare-bones water cycle algorithm for optimal reactive power dispatch in electrical power systems," *Applied Soft Computing*, vol. 57, pp. 657-671, 2017.

[46] P. Anbarasan and T. Jayabarathi, "Optimal reactive power dispatch problem solved by an improved colliding bodies optimization algorithm," in *2017 IEEE International Conference on Environment and Electrical Engineering and 2017 IEEE Industrial and Commercial Power Systems Europe (EEEIC/I&CPS Europe)*, 2017, pp. 1-6: IEEE.

[47] W. M. Villa-Acevedo, J. M. López-Lezama, and J. A. Valencia-Velásquez, "A novel constraint handling approach for the optimal reactive power dispatch problem," *Energies*, vol. 11, no. 9, p. 2352, 2018.

[48] A. M. Shaheen, R. A. El-Sehiemy, and S. M. Farrag, "Integrated strategies of backtracking search optimizer for solving reactive power dispatch problem," *IEEE Systems Journal*, vol. 12, no. 1, pp. 424-433, 2016.

[49] K. Nuaekaew, P. Artrit, N. Pholdee, and S. Bureerat, "Optimal reactive power dispatch problem using a two-archive multi-objective grey wolf optimizer," *Expert Systems with Applications*, vol. 87, pp. 79-89, 2017.

[50] R. P. Singh, V. Mukherjee, and S. Ghoshal, "Optimal reactive power dispatch by particle swarm optimization with an aging leader and challengers," *Applied Soft Computing*, vol. 29, pp. 298-309, 2015.

[51] M. Mehdinejad, B. Mohammadi-Ivatloo, R. Dadashzadeh-Bonab, and K. Zare, "Solution of optimal reactive power dispatch of power systems using hybrid particle swarm optimization and imperialist competitive algorithms," *International Journal of Electrical Power & Energy Systems*, vol. 83, pp. 104-116, 2016.

[52] S. Mouassa and T. Bouktir, "Multi-objective ant lion optimization algorithm to solve large-scale multi-objective optimal reactive power dispatch problem," *COMPEL-The international journal for computation and mathematics in electrical and electronic engineering*, vol. 38, no. 1, pp. 304-324, 2019.

[53] B. Shaw, V. Mukherjee, and S. Ghoshal, "Solution of reactive power dispatch of power systems by an opposition-based gravitational search algorithm," *International Journal of Electrical Power & Energy Systems*, vol. 55, pp. 29-40, 2014.

[54] M. H. Ali, A. M. A. Soliman, M. Abdeen, T. Kandil, A. Y. Abdelaziz, and A. El-Shahat, "A Novel Stochastic Optimizer Solving Optimal Reactive Power Dispatch Problem Considering Renewable Energy Resources," *Energies*, vol. 16, no. 4, 2023.

[55] S. P and R. PN, "Optimal reactive power dispatch using self-adaptive real coded genetic algorithm," *Electr Power Syst Res*, vol. 79, no. 2, pp. 374-381, 2009.

[56] A. H. Khazali and M. Kalantar, "Optimal reactive power dispatch based on harmony search algorithm," *International Journal of Electrical Power & Energy Systems*, vol. 33, no. 3, pp. 684-692, 2011.

[57] G. Chen, L. Liu, Z. Zhang, and S. Huang, "Optimal reactive power dispatch by improved GSA-based algorithm with the novel strategies to handle constraints," *Applied Soft Computing*, vol. 50, pp. 58-70, 2017.

[58] Z. Sahli, A. Hamouda, A. Bekrar, and D. Trentesaux, "Reactive power dispatch optimization with voltage profile improvement using an efficient hybrid algorithm," *Energies*, vol. 11, no. 8, 2018.

[59] M. Tuba and N. Bacanin, "Improved seeker optimization algorithm hybridized with firefly algorithm for constrained optimization problems," *Neurocomputing*, vol. 143, pp. 197-207, 2014.

[60] M. Ettappan, V. Vimala, S. Ramesh, and V. Thiruppathy Kesavan, "Optimal reactive power dispatch for real power loss minimization and voltage stability enhancement using Artificial Bee Colony Algorithm,," *Microprocessors and Microsystems,*, vol. 76, 2020.

[61] S. Sarhan, A. Shaheen, R. El-Sehiemy, and M. Gafar, "An Augmented Social Network Search Algorithm for Optimal Reactive Power Dispatch Problem," *Mathematics*, vol. 11, no. 5, 2023.

[62] B. Shaw, V. Mukherjee, and S. P. Ghoshal, "Solution of reactive power dispatch of power systems by an opposition-based gravitational search algorithm.," *Int. J. Electr. Power Energy Syst*, vol. 55, pp. 29-40, 2014.

[63] A. A. Heidari, R. Ali Abbaspour, and A. Rezaee Jordehi, "Gaussian bare-bones water cycle algorithm for optimal reactive power dispatch in electrical power systems," *Appl. Soft Comput. J.* , vol. 57, pp. 657-671, 2017.

[64] Hassan, M. H., Kamel, S., Alateeq, A., Alassaf, A., & Alsaleh, I. (2023). Optimal Power Flow Analysis with Renewable Energy Resource Uncertainty: A Hybrid AEO-CGO Approach. *IEEE Access*.

[65] Dehghani, M., Hubálovský, Š., & Trojovský, P. (2021). Northern goshawk optimization: a new swarm-based algorithm for solving optimization problems. *Ieee Access*, *9*, 162059-162080.

[66] Trojovský, P., & Dehghani, M. (2022). Pelican optimization algorithm: A novel nature-inspired algorithm for engineering applications. *Sensors*, *22*(3), 855.